Capacity Analysis of MIMO Systems Using Limited Feedback Transmit Precoding Schemes

Jun Zheng, *Student Member, IEEE*, and Bhaskar D. Rao, *Fellow, IEEE*

Abstract—This paper employs a high resolution quantization framework to study the effects of finite-rate feedback of the channel state information (CSI) on the performance of multiple-input–multiple-output (MIMO) systems over independently and identically distributed (i.i.d.) Rayleigh flat fading channels. The contributions of this paper are twofold. First, we extend the general distortion analysis of vector quantizers to deal with complex source variables. Necessary and sufficient conditions that guarantee a concise high-resolution distortion analysis in the complex domain is presented. Second, as an application of the proposed complex distortion analysis, tight lower bounds on the capacity loss due to the finite-rate channel quantization are provided for MIMO systems employing a fixed number of equal power spatial beams. Based on the obtained closed-form analytical results, it is shown that the system capacity loss decreases exponentially as the ratio of the quantization rate to the total degrees of freedom of the channel state information to be quantized. Moreover, MIMO CSI-quantizers using mismatched codebooks that are only optimized for high-signal-to-noise ratio (SNR) and low-SNR regimes are also investigated to quantify the penalties incurred by the use of mismatched codebooks. In addition, the analysis is extended to deal with MIMO systems using multi-mode spatial multiplexing transmission schemes with finite-rate CSI feedback. Finally, numerical and simulation results are presented which confirm the tightness of the derived theoretical distortion bounds.

Index Terms—Bennetts integral, capacity analysis, channel quantization, channel state information (CSI) feedback, complex distortion analysis, constrained source, finite-rate feedback, high-resolution quantization theory, imperfect CSIT, mismatched channel quantizer, multiple-input multiple-output (MIMO), transmit precoding, vector quantization.

I. INTRODUCTION

THIS PAPER considers multiple-input–multiple-output (MIMO) systems with partial channel state information (CSI) conveyed to the transmitter by the receiver through a finite-rate feedback link. Recently, several interesting papers have appeared proposing design algorithms as well as analytical results quantifying the performance of finite-rate feedback multiple antenna systems [1]–[7], [8]–[19], [20]. The analysis is quite involved and several approaches have been developed for this purpose in these papers.

By utilizing the geometrical properties of the channel space (vector space of the channel state information), Mukkavilli *et al.* [1] approximated the channel quantization regions and derived a universal lower bound on the outage probability of quantized multiple-input–single-output (MISO) beamforming systems with arbitrary number of transmit antennas t over independently and identically distributed (i.i.d.) Rayleigh fading channels. The approach taken by Love *et al.* in [2]–[4] is based on relating the problem to that of Grassmannian line packing [5]. By utilizing the results on the density of Grassmannian line packings, the authors developed bounds on the codebook size given a capacity or signal-to-noise ratio (SNR) loss for both MISO and MIMO systems. Dai *et al.* [6] took a similar approach and derived a closed-form formula for the volume of a Grassmannian metric ball, which is defined as a closed region of points whose chordal distance with respect to (w.r.t.) the center point is smaller than its radius. Tight lower and upper bounds of the distortion rate tradeoff were established and applied to derive the capacity of a MIMO system with finite-rate CSI feedback. Love *et al.* also investigated in [7] the problem of quantizing the beamforming vector in the context of equal gain transmission, i.e., beamforming under a per-antenna power constraint. The problem of quantized equal gain transmission was recently revisited by Murthy *et al.* wherein a VQ approach was suggested for codebook design [8] and a closed-form capacity loss analysis was conducted.

Another approach is based on identifying and approximating the statistical distribution of the key random variable that characterizes the system performance. This approach was used by Xia *et al.* in [9] and [10], by Zhou *et al.* in [11], and by Roh *et al.* in [12], where the authors first derived an (weighted) inner product criterion and used the Lloyd algorithm [13] to generate the codebook. These works analyzed the performance of MISO systems with limited rate-feedback in the case of i.i.d. Rayleigh fading channels, and obtained closed-form expressions of the capacity loss (or SNR loss) in terms of feedback rate B and antenna size t. In [14] and [15], the results were extended from MISO channels to the case of MIMO systems with quantized feedback. Another analysis approach adopted by Narula *et al.* in [16] is based on relating the quantization problem to rate distortion theory. An approximation of the expected loss of the received SNR due to finite-rate quantization of the beamforming vectors is derived in an MISO system with a large number of antennas t.

J. Zheng is with the Department of Electrical and Computer Engineering, University of California at San Diego, La Jolla, CA 92093-0407 USA, and also with the Broadcom Corporation, 16340 West Bernardo Drive, San Diego, CA 92127 (e-mail: juzheng@ucsd.edu; junz@broadcom.com).

B. D. Rao is with the Department of Electrical and Computer Engineering, University of California at San Diego, La Jolla, CA 92093-0407 USA (e-mail: brao@ece.ucsd.edu).

Despite recent progress, the analysis of finite-rate feedback systems has proven to be difficult and many open issues remain. All the previously described works are case specific, limited to i.i.d. channels, mainly MISO channels, and are difficult to extend to more general scenarios. Recently, in our work [21], a general framework for the analysis of quantized feedback multiple antenna systems was developed using a source coding perspective by leveraging the considerable work that exists in this area, particularly high resolution quantization theory. Specifically, the channel quantization was formulated as a general finite-rate vector quantization problem with attributes tailored to meet the general issues that arise in feedback based communication systems, including encoder side information, source vectors with constrained parameterizations, and general non-mean-squared distortion functions. Asymptotic distortion analysis of the proposed general quantization problem was provided by extending Bennett's classic analysis [22] as well as its corresponding vector extensions [23], [24]. By using the proposed general framework, performance analysis of a feedback-based MISO beamforming system over i.i.d. and correlated Rayleigh flat fading channels was provided in [25]. Moreover, as extended applications of the proposed framework, suboptimal CSI quantizers using mismatched codebooks and transformed codebooks were also investigated in [26]. Related analytical approach from the source coding perspective was also investigated by Mondal *et al.* in [27], where the problem of quantization in an Euclidean space with constraints is converted into an unconstrained quantization problem on an appropriate manifold. By using the proposed lower bound of the distortion rate function, capacity analysis of MISO systems with finite-rate CSI feedback was provided in [27], which is consistent with the results obtained in [12] and [21]. In this paper, by building upon the results from [21] and [25], we further extend the capacity (or capacity loss) analysis from MISO systems to MIMO systems with finite-rate CSI feedback. The material of this paper was partly presented in conference [28].

The contributions of this paper are twofold. First, we extend the general distortion analysis of vector quantizers to deal with complex source variables. Necessary and sufficient conditions that guarantee a concise high-resolution distortion analysis in the complex domain are presented. Second, as an application of the proposed complex distortion analysis, this paper investigates the effects of finite-rate CSI quantization on MIMO systems over i.i.d. Rayleigh flat fading channels. More specifically, tight lower bounds of the average asymptotic distortion, which is defined as the system capacity loss due to the finite-rate channel quantization, are provided for MIMO systems employing a fixed number of equal power spatial beams. Based on the obtained closed-form analytical results, it is shown that the system capacity loss decreases as $\mathcal{O}(2^{-B/(tn-n^2)})$, where B is the number of feedback bits, t is the number of transmit antennas, and n is number of active spatial beams used by the precoder. This result reveals an interesting fact that the exponential decreasing rate of the system capacity loss is two times the ratio of the quantization rate to the total degrees of freedom of the channel state information to be quantized, which is $2tn - 2n^2$. MIMO CSI-quantizers with mismatched codebooks that are only optimized for high-SNR and low-SNR regimes are also investigated and the performance analysis quantifies the penalties incurred by the mismatched CSI-quantizers. As an extension of the distortion analysis, the performance of MIMO systems using the more general multi-mode spatial multiplexing transmission schemes with finite-rate CSI feedback is also provided. Finally, numerical and simulation results are presented which confirm the tightness of the theoretical distortion bounds.

II. DISTORTION ANALYSIS OF THE GENERALIZED COMPLEX VECTOR QUANTIZER

Multiple antenna systems with finite-rate feedback were formulated in [21] as a generalized vector quantization problem with additional attributes such as encoder side information, constrained quantization variable and non-mean-squared distortion measures. High resolution tools commonly used in classical vector quantizations were extended to deal with this generalized problem [21], [25]. The proposed distortion analysis was initially developed for source variables in the real domain. However, in most communication systems, the CSI to be quantized is usually represented as a complex vector or complex matrix. Therefore, in order to apply the asymptotic distortion analysis provided in [21] to these situations, one always has to transform complex sources into real vectors by expanding their real and imaginary parts. However, this makes the analysis cumbersome and more importantly valuable insight is lost as the structure inherent in the problem is obfuscated. An analysis directly using complex variables is beneficial based on experience from other areas, e.g., adaptive filtering. Fortunately, under certain necessary and sufficient conditions, it is shown that the proposed distortion analysis can be performed in the complex domain directly without increasing the vector size (due to the transformation) significantly reducing the complexity of the analysis. Utilizing the general framework in [21], we extend the asymptotic distortion analysis of the generalized vector quantizer for complex source variables. Due to space limitations, we only summarize some of the important results in this section (please refer to [29] for more details). The obtained distortion analysis is then utilized to investigate MIMO systems with finite-rate CSI feedback in Section IV.

A. Problem Formulation

It is assumed that the source variable $\mathbf{x}$ is a two-vector tuple denoted as $(\mathbf{y}, \mathbf{z})$, where $\mathbf{y} \in \mathbb{Q}$ ($\mathbb{Q} \triangleq \mathbb{C}^{k_q}$) is a complex vector of size $k_q \times 1$ representing the actual quantization variable (of $2k_q$ real degrees of freedom) and $\mathbf{z} \in \mathbb{Z}$ is the additional side information. The *side information* $\mathbf{z}$ is available at the encoder (receiver) but not at the decoder (transmitter). The concept of side information is important especially for channel feedback problems because not all the channel parameters need to be quantized. For example, consider a $t \times 1$ MISO system using quantized maximum ratio transmission (MRT) scheme. The optimal beamforming vector is the channel directional vector $\mathbf{v} = \mathbf{h}/\|\mathbf{h}\|$ [30], where $\mathbf{h}$ is $t \times 1$ vector representing the channel response. In this case, the gain of the MISO channel $\|\mathbf{h}\|$ is not quantized, but can be utilized as side information at the quantizer to improve the quantization performance.

Quantization variable $\mathbf{y}$ and side information $\mathbf{z}$ have joint probability density function[1] given by $p(\mathbf{y}, \mathbf{z})$ and a fixed-rate (B bits) quantizer with $N = 2^B$ quantization levels is considered. Based on a particular source realization $\mathbf{x}$, the encoder (or the quantizer) represents complex vector $\mathbf{y}$ by one of the N vectors $\hat{\mathbf{y}}_1, \hat{\mathbf{y}}_2, \ldots, \hat{\mathbf{y}}_N$, which form the codebook. The encoding or the quantization process is denoted as $\hat{\mathbf{y}} = \mathcal{Q}(\mathbf{y}, \mathbf{z})$. The average distortion of a finite-rate quantizer is defined as

$$D = E_{\mathbf{x}}[D_{\mathrm{Q}}(\mathbf{y}, \hat{\mathbf{y}}; \mathbf{z})] \qquad (1)$$

where $D_{\mathrm{Q}}(\mathbf{y}, \hat{\mathbf{y}}; \mathbf{z})$ is a general *non-mean-squared* distortion function between $\mathbf{y}$ and $\hat{\mathbf{y}}$ that is parameterized by $\mathbf{z}$. The distortion function $D_{\mathrm{Q}}(\mathbf{y}, \hat{\mathbf{y}}; \mathbf{z})$ is assumed to be a real function and so is not analytic calling for the use of Wirtinger Calculus [31]. It is assumed to have continuous second-order derivatives w.r.t. to the real and imaginary components of $\mathbf{y}$. By utilizing Wirtinger Calculus together with the local minima assumption of D_{Q} w.r.t. $\mathbf{y}$ at point $\mathbf{y} = \hat{\mathbf{y}}$, we have D_{Q} and its first-order derivative evaluated at $\mathbf{y} = \hat{\mathbf{y}}$ being zero leading to the following second-order Taylor series approximation of the distortion function [32]:

$$\begin{aligned} D_{\mathrm{Q}}(\mathbf{y}, \hat{\mathbf{y}}; \mathbf{z}) \approx &(\mathbf{y} - \hat{\mathbf{y}})^{\mathsf{H}} \mathbf{W}_{\mathbf{z}}(\hat{\mathbf{y}}) (\mathbf{y} - \hat{\mathbf{y}}) \\ &+ \Re[(\mathbf{y} - \hat{\mathbf{y}})^{\mathsf{T}} \mathbf{W}'_{\mathbf{z}}(\hat{\mathbf{y}}) (\mathbf{y} - \hat{\mathbf{y}})] \end{aligned} \qquad (2)$$

where $\mathbf{W}_{\mathbf{z}}(\hat{\mathbf{y}}), \mathbf{W}'_{\mathbf{z}}(\hat{\mathbf{y}}) \in \mathbb{C}^{k_{\mathrm{q}} \times k_{\mathrm{q}}}$ are complex Hessian matrices with the (i, j)th element given by

$$\begin{aligned} w_{i,j} &= \left. \frac{\partial^2}{\partial y_i^* \partial y_j} D_{\mathrm{Q}}(\mathbf{y}, \hat{\mathbf{y}}; \mathbf{z}) \right|_{\mathbf{y}=\hat{\mathbf{y}}} \\ w'_{i,j} &= \left. \frac{\partial^2}{\partial y_i \partial y_j} D_{\mathrm{Q}}(\mathbf{y}, \hat{\mathbf{y}}; \mathbf{z}) \right|_{\mathbf{y}=\hat{\mathbf{y}}} \end{aligned} \qquad (3)$$

with y_i^* representing the complex conjugate of y_i. After some manipulations, one can show that the Hessian matrix $\mathbf{W}'_{\mathbf{z}}(\hat{\mathbf{y}})$ equals to zero, if the following conditions are true:

$$\begin{aligned} \left. \frac{\partial^2}{\partial y_{i,\mathrm{R}} \partial y_{j,\mathrm{R}}} D_{\mathrm{Q}}(\mathbf{y}, \hat{\mathbf{y}}; \mathbf{z}) \right|_{\mathbf{y}=\hat{\mathbf{y}}} &= \left. \frac{\partial^2}{\partial y_{i,\mathrm{I}} \partial y_{j,\mathrm{I}}} D_{\mathrm{Q}}(\mathbf{y}, \hat{\mathbf{y}}; \mathbf{z}) \right|_{\mathbf{y}=\hat{\mathbf{y}}} \\ \left. \frac{\partial^2}{\partial y_{i,\mathrm{R}} \partial y_{j,\mathrm{I}}} D_{\mathrm{Q}}(\mathbf{y}, \hat{\mathbf{y}}; \mathbf{z}) \right|_{\mathbf{y}=\hat{\mathbf{y}}} &= \left. -\frac{\partial^2}{\partial y_{i,\mathrm{I}} \partial y_{j,\mathrm{R}}} D_{\mathrm{Q}}(\mathbf{y}, \hat{\mathbf{y}}; \mathbf{z}) \right|_{\mathbf{y}=\hat{\mathbf{y}}} \end{aligned} \qquad (4)$$

where $y_{i,\mathrm{I}}$ and $y_{i,\mathrm{R}}$ are real and imaginary parts of $\mathbf{y}_i$. Intuitively speaking, the condition described in (4) characterizes the second-order symmetric dependency of the distortion function D_{Q} w.r.t. the real and imaginary parts of $\mathbf{y}$, i.e., they are invariant under the operation of switching the real and imaginary parts of the input variables. Fortunately enough, most communication related functions, including the particular example considered in this paper (in Sections III and IV) satisfy this property, e.g., MIMO capacity, the mean square estimation error of the transmitted symbols as a function of the channel response. Therefore, the symmetric dependence condition given by (4) is

[1]$p(\mathbf{y}, \mathbf{z})$ is an abuse of notation, which represents the joint probability density function of four real vectors (real and imaginary parts of $\mathbf{y}$ and $\mathbf{z}$). The multi-dimensional integration (w.r.t. to vectors $\mathbf{y}$ and $\mathbf{z}$) in (6) is also over these four real vectors.

assumed in the rest of this paper, unless specified otherwise. In these cases, the distortion function D_{Q} has a simplified Taylor series expansion given by

$$D_{\mathrm{Q}}(\mathbf{y}, \hat{\mathbf{y}}; \mathbf{z}) \approx (\mathbf{y} - \hat{\mathbf{y}})^{\mathsf{H}} \mathbf{W}_{\mathbf{z}}(\hat{\mathbf{y}}) (\mathbf{y} - \hat{\mathbf{y}}) \qquad (5)$$

where $\mathbf{W}_{\mathbf{z}}(\hat{\mathbf{y}})$ is called the *complex sensitivity matrix*.

B. Asymptotic Distortion Integral

In order to obtain the distortion analysis of a finite-rate quantized k_{q}-dimensional complex source, a transformation from the complex domain into the real domain (by expanding the real and imaginary parts of the source vector) is performed first. Appropriate real dimensionality (which is $2k_{\mathrm{q}}$) and other corresponding quantities are then substituted into the real distortion analysis provided in [21, Sec. II]. Due to the imposed symmetricity of the distortion functions given by (5), the asymptotic distortion of complex sources can *still* be represented in the following concise format:[2]

$$\begin{aligned} D &= E[D_{\mathrm{Q}}(\mathbf{y}, Q(\mathbf{y}, \mathbf{z}); \mathbf{z})] \\ &= \left(\int_{\mathbb{Z}} \int_{\mathbb{Q}} I(\mathbf{y}; \mathbf{z}; \mathbb{E}_{\mathbf{z}}(\mathbf{y})) p(\mathbf{y}, \mathbf{z}) \lambda(\mathbf{y})^{-\frac{1}{k_{\mathrm{q}}}} d\mathbf{y} d\mathbf{z} \right) 2^{-\frac{B}{k_{\mathrm{q}}}} \end{aligned} \qquad (6)$$

where $\mathbb{E}_{\mathbf{z}}(\mathbf{y})$ denotes the asymptotic projected Voronoi cell centered at $\mathbf{y}$ with side information $\mathbf{z}$. It is an infinitesimal region that captures the shape attribute of the quantization cell in the asymptotic sense $(B \to \infty)$. In (6), $\lambda(\mathbf{y})$ is a function representing the relative density of the codepoints (or the Voronoi cell centers), also referred to as the *point density*, such that $\lambda(\mathbf{y})d\mathbf{y}$ is approximately the fraction of quantization points in a small neighborhood of $\mathbf{y}$. Function $I(\mathbf{y}; \mathbf{z}; \mathbb{E}_{\mathbf{z}}(\mathbf{y}))$ is the *normalized inertial profile* that represents the asymptotic normalized distortion of the quantizer $\mathcal{Q}$ at position $\mathbf{y}$ conditioned on side information $\mathbf{z}$ with Voronoi shape $\mathbb{E}_{\mathbf{z}}(\mathbf{y})$. It is defined as[3]

$$\begin{aligned} I(\mathbf{y}; \mathbf{z}; \mathbb{E}_{\mathbf{z}}(\mathbf{y})) \triangleq &\left(\int_{\mathbf{y}' \in \mathbb{E}_{\mathbf{z}}(\mathbf{y})} d\mathbf{y}' \right)^{-\frac{1+k_{\mathrm{q}}}{k_{\mathrm{q}}}} \\ &\times \left(\int_{\mathbf{y}' \in \mathbb{E}_{\mathbf{z}}(\mathbf{y})} (\mathbf{y}' - \mathbf{y})^{\mathsf{H}} \mathbf{W}_{\mathbf{z}}(\mathbf{y}) (\mathbf{y}' - \mathbf{y}) d\mathbf{y}' \right). \end{aligned} \qquad (7)$$

Intuitively speaking, the inertial profile represents the average distortion, which corresponds to the second term on the right-hand side of (7), of an infinitesimal region with proper normalization. The purpose of the normalization w.r.t. the cell volume, which corresponds to the first term on the right-hand side of (7), is to make sure the inertial profile is invariant under arbitrary scalings of the cell. Therefore, the inertial profile depends only on the cell shape and the sensitivity matrix at a specific location, but not the cell size. It characterizes the local (or finer) quality

[2]Having a concise distortion analysis directly applicable in the complex domain is especially important for source variables with large dimensions, for example finite-rate quantization of MIMO channels. This is because the analysis becomes more cumbersome and much more complicated when the dimensionality is doubled (performing analysis in the real domain after expanding).

[3]Compared with the distortion analysis of real source variables provided in [21], the integrations w.r.t. $\mathbf{y}$ and $\mathbf{y}'$ in (6) and (7) are over regions $\mathbb{Q}$ and $\mathbb{E}_{\mathbf{z}}(\mathbf{y})$ with $2k_{\mathrm{q}}$ real dimensions respectively.

of a high resolution quantizer, in terms of relative distortion, at different locations and with different cell shapes.

Finally, note that the point density function $\lambda(\mathbf{y})$ and the normalized inertial profile $I(\mathbf{y}; \mathbf{z}; \mathbb{E}_{\mathbf{z}}(\mathbf{y}))$ are the key functions that describe the behavior of a specific quantizer. Hence, given a vector quantizer, the problem reduces to finding these two functions and the average system distortion can be obtained by substituting them into the distortion integral given by (6) [21].

C. Characterizing the Normalized Inertial Profile

The normalized inertial profile of an optimal quantizer is defined as the minimum inertia of all admissible regions $\mathbb{E}_{\mathbf{z}}(\mathbf{y})$, i.e.,

$$I_{\text{opt}}(\mathbf{y}; \mathbf{z}) \triangleq \min_{\mathbb{E}_{\mathbf{z}}(\mathbf{y}) \in \mathcal{H}_Q} I(\mathbf{y}; \mathbf{z}; \mathbb{E}_{\mathbf{z}}(\mathbf{y})) \qquad (8)$$

where $\mathcal{H}_Q$ represents the set of all admissible tessellating polytopes that can tile the quantization space $\mathbb{Q}$ with $2k_q$ real dimensions. It is known that finding the optimal Voronoi region as well as characterizing the exact optimal inertial profile is hard. However, similar to the case of real source variables, the inertial profile of any complex Voronoi shape $\mathbb{E}_{\mathbf{z}}(\mathbf{y})$, including the optimal inertial profile, can be tightly lower bounded by using a complex "M-shaped" hyper-ellipsoidal Voronoi shape. A *complex* hyper-ellipsoid[4] $\mathcal{T}(\mathbf{y}, \mathbf{M}, v)$ can be defined as the following form:

$$\mathcal{T}(\mathbf{y}, \mathbf{M}, v) = \left\{ \mathbf{x} \in \mathbb{C}^{k_q \times 1} \middle| \left(\frac{\kappa_{2k_q}}{v|\mathbf{M}|} \right)^{\frac{1}{k_q}} \right.$$
$$\left. \times (\mathbf{x} - \mathbf{y})^{\mathsf{H}} \mathbf{M} (\mathbf{x} - \mathbf{y}) \leq 1 \right\}$$
$$\kappa_n = \frac{\pi^{n/2}}{\Gamma(n/2 + 1)} \qquad (9)$$

where $|\cdot|$ represents matrix determinant and v represents the volume (or area) of the hyper-ellipsoid. Positive definite matrix $\mathbf{M}$ in (9) is called the coordinate matrix of the hyper-ellipsoid whose eigen-decomposition gives the lengths (the eigen-values) of the principal axes and their orientations (the rotation specified by the eigen-vectors). It was shown in [24] that among all possible hyper-ellipsoids, the one with coordinate matrix $\mathbf{M}$ equal to the complex sensitivity matrix $\mathbf{W}_{\mathbf{z}}(\mathbf{y})$ achieves the minimal inertial profile. Therefore, by setting $\mathbf{M} = \mathbf{W}_{\mathbf{z}}(\mathbf{y})$ and substituting the definition of the hyper-ellipsoid (9) into the inertial profile definition given by (7), a *tight* lower bound [24],

[4]The *complex* hyper-ellipsoid is a straightforward extension of the concept of real hyper-ellipsoid [33]. To be specific, complex hyper-ellipsoid $\mathcal{T}(\mathbf{y} \in \mathbb{C}^{k_q}, \mathbf{M}, v)$ is equivalent to real hyper-ellipsoid $\mathcal{T}(\bar{\mathbf{y}} \in \mathbb{R}^{2k_q}, \mathbf{M}_{\text{eq}}, v^2)$ with $\bar{\mathbf{y}} = [\mathbf{y}_R^{\mathsf{T}}, \mathbf{y}_I^{\mathsf{T}}]^{\mathsf{T}}$ and

$$\mathbf{M}_{\text{eq}} = \begin{bmatrix} \mathbf{M}_R & -\mathbf{M}_I \\ \mathbf{M}_I & \mathbf{M}_R \end{bmatrix}$$

where $\mathbf{y}_R, \mathbf{y}_I, \mathbf{M}_R, \mathbf{M}_I$ are the real and imaginary parts of $\mathbf{y}$ and $\mathbf{M}$, respectively.

[34] of the complex inertial profile can be obtained after some manipulations:[5]

$$\begin{aligned} I(\mathbf{y}; \mathbf{z}; \mathbb{E}_{\mathbf{z}}(\mathbf{y})) &\geq I_{\text{opt}}(\mathbf{y}; \mathbf{z}) \\ &\gtrsim \tilde{I}_{\text{opt}}(\mathbf{y}; \mathbf{z}) \\ &= I(\mathbf{y}; \mathbf{z}; \mathcal{T}(\mathbf{y}, \mathbf{W}_{\mathbf{z}}(\mathbf{y}), v)) \\ &= \frac{k_q}{k_q + 1} \left(\frac{|\mathbf{W}_{\mathbf{z}}(\mathbf{y})|}{\kappa_{2k_q}} \right)^{\frac{1}{k_q}}. \end{aligned} \qquad (10)$$

D. Asymptotic Distortion Bounds

Under high resolution assumptions, the average distortion of a generalized finite-rate quantization system for complex source variables can be lower bounded by the following form:

$$D_{\text{Opt}} \geq D_{\text{Low}} = \left(\int_{\mathbb{Q}} \left(I_{\text{opt}}^{\text{w}}(\mathbf{y}) p(\mathbf{y}) \right)^{\frac{k_q}{1+k_q}} d\mathbf{y} \right)^{\frac{1+k_q}{k_q}} 2^{-\frac{B}{k_q}} \qquad (11)$$

where $I_{\text{opt}}^{\text{w}}(\mathbf{y})$ is the average optimal inertial profile defined as

$$I_{\text{opt}}^{\text{w}}(\mathbf{y}) = \int_{\mathbb{Z}} I_{\text{opt}}(\mathbf{y}; \mathbf{z}) p(\mathbf{z} \,|\, \mathbf{y}) \, d\mathbf{z}. \qquad (12)$$

Equation (11) can be obtained from (6) by using $I_{\text{opt}}^{\text{w}}(\mathbf{y})$ given above and selecting the point density function optimally to minimize the asymptotic system distortion, i.e., [21]

$$\lambda^*(\mathbf{y}) = \left(I_{\text{opt}}^{\text{w}}(\mathbf{y}) p(\mathbf{y}) \right)^{\frac{k_q}{1+k_q}} \left(\int_{\mathbb{Q}} \left(I_{\text{opt}}^{\text{w}}(\mathbf{y}) p(\mathbf{y}) \right)^{\frac{k_q}{1+k_q}} d\mathbf{y} \right)^{-1}. \qquad (13)$$

Moreover, by substituting the tight lower bound (10) of the inertial profile into (11), one can obtain corresponding tight lower bounds of the average inertial profile $\tilde{I}_{\text{opt}}^{\text{w}}(\mathbf{y})$, point density $\tilde{\lambda}^*(\mathbf{y})$, as well as asymptotic distortion bounds $\tilde{D}_{\text{Low}}$, respectively.[6]

E. Distortion Analysis of Constrained Source

Compared with conventional source coding problems, where the input source variables are free random vectors, the quantized variable in feedback wireless systems are often constrained. For example, consider a $t \times 1$ MISO quantized MRT beamforming system, the beamforming vector $\mathbf{v} \in \mathbb{C}^t$ to be quantized is constrained to be unit-norm and hence lies on the unit hyper-sphere or manifold, whereas the channel instantiation $\mathbf{h}$ is a general vector in $\mathbb{C}^t$ space. For the quantized MIMO precoding problem discussed in this paper, the precoding matrix $\mathbf{V}$ to be quantized is also constrained to be unitary matrices. Therefore, it is both of great importance and also very interesting to study the finite-rate quantization of source variables subject to a multi-dimensional

[5]The derivation of the complex inertial profile lower bound is a straightforward extension of the lower bound for real source variables. It can be obtained by first converting the dimensionality from k_q (complex) into $2k_q$ (real) and using a real coordinate matrix given by

$$\begin{bmatrix} \mathbf{W}_{\mathbf{z}}(\hat{\mathbf{y}})_R & -\mathbf{W}_{\mathbf{z}}(\hat{\mathbf{y}})_I \\ \mathbf{W}_{\mathbf{z}}(\hat{\mathbf{y}})_I & \mathbf{W}_{\mathbf{z}}(\hat{\mathbf{y}})_R \end{bmatrix}$$

according to discussion given by footnote 4.

[6]This replacement can be extended to other variables and definitions. In the rest of this paper, we will directly use $\bar{a}$ to represent a quantity that is obtained by replacing I_{opt} with $\tilde{I}_{\text{opt}}$ when a is a function of I_{opt}, i.e., $a = a(I_{\text{opt}})$.

real constraint function $\mathbf{g}(\mathbf{y}) = \mathbf{0}$. To be specific, suppose the constraint function $\mathbf{g}(\mathbf{y})$ is of size $2k_c \times 1 (k_c \le k_q)$ and can be partitioned into the following form under proper orderings[7]

$$\mathbf{g}(\mathbf{y}) = \left[\mathbf{g}_1^\top(\mathbf{y})\mathbf{g}_2^\top(\mathbf{y})\right]^\top \quad \mathbf{g}_1(\mathbf{y}), \mathbf{g}_2(\mathbf{y}) \in \mathbb{R}^{k_c \times 1}.$$

It is shown in [21] that the asymptotic distortion analysis derived for unconstrained source vectors is still valid for constrained sources with appropriate modifications. The following proposition states the necessary and sufficient condition for the inertial profile of the complex constrained source to have a concise format similar to the real case.

Proposition 1: The normalized inertial profile of the constrained complex source $\mathbf{y}$ can be represented by the following form:

$$I_c(\hat{\mathbf{y}}_i; \mathbf{z}; \mathbb{E}_{\mathbf{z},i}) = V(\mathbb{E}_{\mathbf{z},i})^{-(1+\frac{1}{k_q'})} \int_{\mathbf{e} \in \mathbb{E}_{\mathbf{z},i}^c} \mathbf{e}^\mathsf{H} \mathbf{W}_{c,\mathbf{z}}(\hat{\mathbf{y}}_i)\mathbf{e}\, d\mathbf{e} \tag{14}$$

where $k_q' = k_q - k_c$, $\mathbb{E}_{\mathbf{z},i}$ is the Voronoi region (shape) that corresponds to code point $\hat{\mathbf{y}}_i$ with side information $\mathbf{z}$, and $V(\mathbb{E}_{\mathbf{z},i})$ represents the volume (or area) of this Voronoi cell. The *constrained sensitivity matrix* $\mathbf{W}_{c,\mathbf{z}}(\hat{\mathbf{y}}_i)$ used in (14) can be represented as

$$\mathbf{W}_{c,\mathbf{z}}(\hat{\mathbf{y}}) = \mathbf{V}_2^\mathsf{H} \mathbf{W}_{\mathbf{z}}(\hat{\mathbf{y}})\mathbf{V}_2 \tag{15}$$

with the unconstrained sensitivity matrix $\mathbf{W}_{\mathbf{z}}(\hat{\mathbf{y}})$ given by (3) and matrix $\mathbf{V}_2$ being an orthonormal matrix whose columns constitute an orthonormal basis for the null space $\mathcal{N}((\partial/\partial\mathbf{y})\mathbf{g}_1(\mathbf{y}))$, *if and only if* there exists a non-singular matrix $\boldsymbol{\Phi}$ satisfying the following equation:

$$\frac{\partial \mathbf{g}_1(\tilde{\mathbf{y}}')}{\partial \tilde{\mathbf{y}}'} = \boldsymbol{\Phi} \frac{\partial \mathbf{g}_2(\tilde{\mathbf{y}})}{\partial \tilde{\mathbf{y}}}$$
$$\tilde{\mathbf{y}} = [\mathbf{y}^\top, \mathbf{y}^\mathsf{H}]^\top$$
$$\tilde{\mathbf{y}}' = [-\mathbf{y}^\top, \mathbf{y}^\mathsf{H}]^\top. \tag{16}$$

In this case, the constrained inertial profile can also be tightly lower bounded by the following form:

$$I_{c,\mathrm{opt}}(\hat{\mathbf{y}}_i; \mathbf{z}) \gtrsim \tilde{I}_{c,\mathrm{opt}}(\hat{\mathbf{y}}_i; \mathbf{z})$$
$$= \frac{k_q'}{k_q' + 1}\left(\frac{|\mathbf{W}_{c,\mathbf{z}}(\hat{\mathbf{y}}_i)|}{\kappa_{2k_q'}}\right)^{\frac{1}{k_q'}}. \tag{17}$$

Proof: Please see Appendix A.   ∎

Based upon the results established in Proposition 1, the asymptotic distortion analysis provided in previous subsections for unconstrained source variables can be shown to be valid for constrained sources with the following modification.

[7]The ordering of the constrained conditions (or the elements of vector $\mathbf{g}(\mathbf{y})$) does *not* impact the system performance. However, certain orderings can lead to concise complex distortion analysis, whose necessary and sufficient condition is given by (16) in Proposition 1. Note from (16), there are more than one orderings that can lead to concise analysis, i.e., permutations within $\mathbf{g}_1$ and $\mathbf{g}_2$ still satisfy the condition and hence will also have concise distortion analysis.

First, the complex free dimensions of $\mathbf{y}$ is reduced from k_q to $k_q' = k_q - k_c$. Next, the sensitivity matrix is replaced by its constrained version $\mathbf{W}_{c,\mathbf{z}}(\mathbf{y})$ given by (15) and the constrained normalized inertial profile is defined as (14) and tightly lower bounded by (17). Last, the multi-dimensional integrations used in evaluating the average distortions are over the constrained space $\mathbf{g}(\mathbf{y}) = 0$. Finally, the average system distortion is lower bounded by the following form:

$$D_{\mathrm{Low}} = \left(\int_{\mathbf{g}(\mathbf{y})=0}\left(\tilde{I}_{c,\mathrm{opt}}^{\mathrm{w}}(\mathbf{y})p(\mathbf{y})\right)^{\frac{k_q'}{1+k_q'}}d\mathbf{y}\right)^{\frac{1+k_q'}{k_q'}}2^{-\frac{B}{k_q'}}$$
$$\tilde{I}_{c,\mathrm{opt}}^{\mathrm{w}}(\mathbf{y}) = \int_{\mathbb{Z}}\tilde{I}_{c,\mathrm{opt}}(\mathbf{y};\mathbf{z})p(\mathbf{z}\,|\,\mathbf{y})d\mathbf{z}. \tag{18}$$

F. Analysis of Quantizers With Mismatched Codebooks

In some cases, the quantizer is designed by using a distortion measure that is different from the actual system distortion function D_Q in order to reduce the complexity of the codebook design algorithms. To be specific, the distortion function of interest is denoted by D_Q and the distortion function used for designing the quantizer is denoted by $D_{\mathrm{mis\text{-}Q}}$, whose complex sensitivity matrix is given by $\mathbf{W}_{\mathrm{mis},\mathbf{z}}(\mathbf{y})$. Codebook generated or trained by the mismatched sensitivity matrix has a mismatched Voronoi region $\mathbb{E}_{\mathrm{mis},\mathbf{z}}(\mathbf{y})$, which further leads to a mismatched inertial profile that can be closely approximated by

$$I_{\mathrm{mis\text{-}D}}(\mathbf{y};\mathbf{z}) \approx \tilde{I}_{\mathrm{mis\text{-}D}}(\mathbf{y};\mathbf{z})$$
$$= \frac{1}{k_q + 1}\left(\frac{|\mathbf{W}_{\mathrm{mis},\mathbf{z}}(\mathbf{y})|}{\kappa_{2k_q}}\right)^{\frac{1}{k_q}}$$
$$\times \mathrm{tr}\left(\mathbf{W}_{\mathrm{mis},\mathbf{z}}^{-1}(\mathbf{y})\mathbf{W}_{\mathbf{z}}(\mathbf{y})\right). \tag{19}$$

In addition, the mismatched sensitivity matrix also leads to a mismatched point density function having the following form, from (13):

$$\lambda_{\mathrm{mis\text{-}D}}(\mathbf{y}) = \left(\tilde{I}_{\mathrm{opt\text{-}mis}}^{\mathrm{w}}(\mathbf{y})p(\mathbf{y})\right)^{\frac{k_q}{1+k_q}}$$
$$\times \left(\int_{\mathbb{Q}}\left(\tilde{I}_{\mathrm{opt\text{-}mis}}^{\mathrm{w}}(\mathbf{y})p(\mathbf{y})\right)^{\frac{k_q}{1+k_q}}d\mathbf{y}\right)^{-1} \tag{20}$$

where $\tilde{I}_{\mathrm{opt\text{-}mis}}^{\mathrm{w}}(\mathbf{y})$ is the optimal average inertia profile of a system with actual distortion function equal to $D_{\mathrm{mis\text{-}Q}}$. Finally, by substituting the previous mismatched inertial profile (19) and mismatched point density (20) into the distortion integral given by (6), the average distortion of a quantizer with mismatched distortion function can be obtained as

$$\tilde{D}_{\mathrm{mis\text{-}D}} = \left(\int_{\mathbb{Z}}\int_{\mathbb{Q}}\tilde{I}_{\mathrm{mis\text{-}D}}(\mathbf{y})p(\mathbf{y},\mathbf{z})\right.$$
$$\left. \times \tilde{\lambda}_{\mathrm{mis\text{-}D}}(\mathbf{y})^{-\frac{1}{k_q}}d\mathbf{y}d\mathbf{z}\right)2^{-\frac{B}{k_q}}. \tag{21}$$

III. System Model of MIMO Systems With Finite-Rate Feedback

A. Fading Channel Model

We consider a MIMO system with t transmit antennas and r receive antennas, signaling through a frequency flat Rayleigh fading channel. The channel model can be represented as

$$\mathbf{y} = \mathbf{H} \cdot \mathbf{x} + \mathbf{n} \tag{22}$$

where $\mathbf{y}$ is the received signal, $\mathbf{n}$ is the additive complex Gaussian noise with distribution $\mathcal{N}_c(\mathbf{0}, I_r)$, and $\mathbf{H}$ is the MIMO channel response of size $r \times t$ with each of its element being independent, complex Gaussian distributed with zero mean and unit variance. The transmitted signal vector $\mathbf{x}$ is normalized to have a power constraint given by $E[\|\mathbf{x}\|^2] = \rho$, with ρ representing the average SNR at each receive antenna. With probability one, the MIMO channel matrix $\mathbf{H}$ has rank m equal to the minimum number of the transmit and receive antennas, i.e., $m = \min(t, r)$. The singular value decomposition (SVD) of matrix $\mathbf{H}$ is denoted as $\mathbf{H} = \mathbf{U}_{\mathrm{H}} \mathbf{\Sigma}_{\mathrm{H}}^{(1/2)} \mathbf{V}_{\mathrm{H}}^{\mathsf{H}}$, where $\mathbf{U}_{\mathrm{H}} \in \mathbb{C}^{r \times m}$ and $\mathbf{V}_{\mathrm{H}} \in \mathbb{C}^{t \times m}$ are orthonormal column matrices and $\mathbf{\Sigma}_{\mathrm{H}} = \mathbf{diag}[\lambda_1, \lambda_2, \ldots, \lambda_m]$ is a diagonal matrix with $\lambda_1 \geq \lambda_2 \geq \cdots \geq \lambda_m > 0$ representing the sorted nonzero eigen-values of matrix $\mathbf{H}\mathbf{H}^{\mathsf{H}}$.

B. Transmit Precoding Schemes With Quantized CSIT

The channel state information $\mathbf{H}$ is assumed to be perfectly available at the receiver but only partially known at the transmitter through a finite-rate feedback link of B bits per channel update between the transmitter and the receiver. Moreover, for a given transmission supporting n spatial streams ($n \leq m$), a precoding scheme using equal power allocation among the active spatial streams is adopted [10], [14], [35] in this paper. To be specific, a precoding matrix codebook $\mathcal{C} = \{\hat{\mathbf{F}}_1, \ldots, \hat{\mathbf{F}}_N\}$ is exposed to both the receiver and the transmitter, whose elements are of size $t \times n$ and satisfy the condition: $\hat{\mathbf{F}}_i^{\mathsf{H}} \hat{\mathbf{F}}_i = I_n/n$. Based on the channel realization $\mathbf{H}$, the receiver selects the best code point $\hat{\mathbf{F}}$ from the codebook and transmits the corresponding index back to the transmitter. At the transmitter, the unit-norm matrix $\hat{\mathbf{F}}$ is employed as the precoding matrix, and the resultant received signal can be represented as

$$\mathbf{y} = \mathbf{H}(\hat{\mathbf{F}} \cdot \mathbf{s}) + \mathbf{n} \quad E[\mathbf{s} \cdot \mathbf{s}^{\mathsf{H}}] = \rho \cdot I_n. \tag{23}$$

With perfect channel state information available at the transmitter ($B = \infty$), it is optimal [35] to choose $\hat{\mathbf{F}} = \mathbf{V}/\sqrt{n}$ (under the assumption of using unitary precoding matrix), where matrix $\mathbf{V}$ corresponds to the first n dominant eigen-vectors of $\mathbf{H}^{\mathsf{H}}\mathbf{H}$ (composed of the first n columns of $\mathbf{V}_{\mathrm{H}}$). In this case, the system capacity[8] by using a n-beam transmit precoding scheme with equal power allocation is given by

$$C_{\mathrm{perf}} = E[C_{\mathrm{p}}(\mathbf{H})] = E\left[\log_2 \det\left(I + \frac{\rho}{n}\mathbf{V}^{\mathsf{H}}\mathbf{H}^{\mathsf{H}}\mathbf{H}\mathbf{V}\right)\right]$$
$$= E\left[\log_2 \det\left(I + \frac{\rho}{n}\mathbf{\Sigma}_{\mathrm{H},n}\right)\right] \tag{24}$$

[8]The system capacity here refers to the mutual information rate of a specific setting. The actual capacity without the restriction of equal power allocation among the spatial bemas is presumably larger than the aforementioned mutual information rate.

where $\mathbf{\Sigma}_{\mathrm{H},n}$ is an $n \times n$ diagonal matrix whose diagonal elements are the first (largest) n eigen-values of $\mathbf{H}^{\mathsf{H}}\mathbf{H}$. When the feedback link is restricted to a finite rate of B bits per channel update, the system capacity with finite-rate CSI feedback can be represented as

$$C_{\mathrm{quan}} = E[C_{\mathrm{q}}(\mathbf{H}, \hat{\mathbf{V}})]$$
$$= E\left[\log_2 \det\left(I + \frac{\rho}{n}\hat{\mathbf{V}}^{\mathsf{H}}\mathbf{H}^{\mathsf{H}}\mathbf{H}\hat{\mathbf{V}}\right)\right] \tag{25}$$

where the quantized beamforming matrix $\hat{\mathbf{V}}$ is a function of the current channel realization $\mathbf{H}$, i.e., $\hat{\mathbf{V}} = \hat{\mathbf{V}}(\mathbf{H}) \in \mathcal{C}$. Therefore, the performance of a CSI-feedback-based MIMO system can be characterized by the system capacity loss C_{Loss}, defined as the expectation of the instantaneous capacity loss, i.e.,

$$C_{\mathrm{Loss}} = C_{\mathrm{perf}} - C_{\mathrm{quan}} = E[C_{\mathrm{L}}(\mathbf{H}, \hat{\mathbf{V}})] \tag{26}$$

where the instantaneous capacity loss $C_{\mathrm{L}}(\mathbf{H}, \hat{\mathbf{V}})$ is given by

$$C_{\mathrm{L}}(\mathbf{H}, \hat{\mathbf{V}}) = C_{\mathrm{p}}(\mathbf{H}) - C_{\mathrm{q}}(\mathbf{H}, \hat{\mathbf{V}})$$
$$= \log_2 \det\left(I + \frac{\rho}{n}\mathbf{\Sigma}_{\mathrm{H},n}\right)$$
$$- \log_2 \det\left(I + \frac{\rho}{n}\hat{\mathbf{V}}^{\mathsf{H}}\mathbf{V}_{\mathrm{H}}\mathbf{\Sigma}_{\mathrm{H}}\mathbf{V}_{\mathrm{H}}^{\mathsf{H}}\hat{\mathbf{V}}\right). \tag{27}$$

This performance metric was also used in [14] and [15]. Furthermore, notice that in practical systems, channel errors and feedback delay also exist in the reverse link, which will impact the overall system performance. However, this paper assumes the feedback is error-free and delay-less, and focuses solely on the effect of finite-rate quantization of the channel state information.

IV. Capacity Analysis of MIMO Precoders With Finite-Rate CSI Feedback

The performance analysis of a finite-rate CSI-feedback-based MIMO system using transmit precoding schemes with equal power allocation on multiple spatial beams is challenging because of the complicated nature of the loss function and the complicated channel related random variables.

A. Formulating the MIMO CSI-Quantizer as a General Vector Quantization Problem

In the MIMO context, the source variable to be quantized is the right singular matrix $\mathbf{V}$ of the fading channel response $\mathbf{H}$. It is a complex matrix of size $t \times n$, which contains $k_{\mathrm{q}} = tn$ complex ($2k_{\mathrm{q}}$ real) dimensions. The system distortion function D_{Q} is chosen to be the instantaneous capacity loss C_{L} given by (27). It is shown in Appendix B that D_{Q} (or C_{L}) can be approximated by the following second-order Taylor series expansion:

$$D_{\mathrm{Q}}(\mathbf{V}, \hat{\mathbf{V}}; \mathbf{\Sigma}_{\mathrm{H},n}) = \log_2 \det\left(I + \frac{\rho}{n}\mathbf{\Sigma}_{\mathrm{H},n}\right)$$
$$- \log_2 \det\left(I + \frac{\rho}{n}\mathbf{\Sigma}_{\mathrm{H}}\mathbf{V}_{\mathrm{H}}^{\mathsf{H}}\hat{\mathbf{V}}\hat{\mathbf{V}}^{\mathsf{H}}\mathbf{V}_{\mathrm{H}}\right)$$
$$\approx \frac{1}{\ln 2}\mathbf{tr}\left(\mathbf{V}^{\mathsf{H}}(I - \hat{\mathbf{V}}\hat{\mathbf{V}}^{\mathsf{H}})\mathbf{V}\frac{\rho}{n}\mathbf{\Sigma}_{\mathrm{H},n}\right.$$
$$\left. \times \left(I + \frac{\rho}{n}\mathbf{\Sigma}_{\mathrm{H},n}\right)^{-1}\right). \tag{28}$$

It can be observed from (28) that the distortion function D_{Q} between $\mathbf{V}$ and $\hat{\mathbf{V}}$ is only parameterized by $\mathbf{\Sigma}_{\mathrm{H},n}$, under the

second-order approximation. The diagonal elements of matrix $\Sigma_{\mathrm{H},n}$ represent the first n nonzero eigen-values of matrix $\mathbf{H}^{\mathsf{H}}\mathbf{H}$. Therefore, the encoder side information in this case can be denoted as $\mathbf{z} = \Sigma_{\mathrm{H},n}$ with n degrees of freedom.

In contrast to the conventional quantization problems, the source variable to be quantized in this case is subject to constraints. First of all, according to the SVD definition, matrix $\mathbf{V}$ has orthonormal column vectors, i.e.,

$$\mathbf{V}^{\mathsf{H}}\mathbf{V} = I_n \quad \mathbf{V} \in \mathbb{C}^{t \times n} \tag{29}$$

which corresponds to n^2 real independent constrained equations. Furthermore, the distortion function D_{Q} can also be rewritten in the following form after some manipulations:

$$
\begin{aligned}
&D_{\mathrm{Q}}(\mathbf{V}, \hat{\mathbf{V}}; \Sigma_{\mathrm{H},n}) \\
&= \frac{1}{\ln 2}\mathbf{tr}\left((I - (\mathbf{V}^{\mathsf{H}}\hat{\mathbf{V}})(\mathbf{V}^{\mathsf{H}}\hat{\mathbf{V}})^{\mathsf{H}})\frac{\rho}{n}\Sigma_{\mathrm{H},n} \right. \\
&\qquad \left. \times \left(I + \frac{\rho}{n}\Sigma_{\mathrm{H},n} \right)^{-1} \right).
\end{aligned}
\tag{30}
$$

From (30), it can be observed that the distortion function D_{Q} depends only on the matrix product $\mathbf{V}^{\mathsf{H}}\hat{\mathbf{V}}$ and the encoder side information $\Sigma_{\mathrm{H},n}$. Hence, the distortion function can be denoted as $D_{\mathrm{Q}}(\mathbf{V}^{\mathsf{H}}\hat{\mathbf{V}}; \Sigma_{\mathrm{H},n})$. Moreover, D_{Q} is invariant under any unitary rotations on matrix $\mathbf{V}^{\mathsf{H}}\hat{\mathbf{V}}$ at the right-hand side, i.e.,

$$D_{\mathrm{Q}}(\mathbf{V}^{\mathsf{H}}\hat{\mathbf{V}}\mathbf{Q}_{\mathrm{R}}; \Sigma_{\mathrm{H},n}) = D_{\mathrm{Q}}(\mathbf{V}^{\mathsf{H}}\hat{\mathbf{V}}; \Sigma_{\mathrm{H},n}) \tag{31}$$

where $\mathbf{Q}_{\mathrm{R}}$ is an arbitrary unitary matrix. Suppose matrix product $\mathbf{V}^{\mathsf{H}}\hat{\mathbf{V}}$ has a unique R–Q decomposition given by the following form:

$$\mathbf{P} = \mathbf{V}^{\mathsf{H}}\hat{\mathbf{V}} = \mathbf{R}_{\mathrm{p}}\mathbf{Q}_{\mathrm{p}} \tag{32}$$

where $\mathbf{Q}_{\mathrm{p}}$ is a unitary matrix and $\mathbf{R}_{\mathrm{p}}$ is an upper triangle matrix with real diagonal elements. Hence, for any realization of $\mathbf{V}$ (or $\mathbf{P}$), there always exists a unitary rotation $\mathbf{Q}_{\mathrm{R}} = \mathbf{Q}_{\mathrm{p}}^{\mathsf{H}}$, such that $\mathbf{P}\mathbf{Q}_{\mathrm{R}}$ is an upper triangle matrix. Therefore, without loss of generality, one can impose on matrix $\mathbf{P}$ the following constraints, such that for points $\mathbf{V}$ in the small neighborhood of $\hat{\mathbf{V}}$, matrix $\mathbf{P}$ is an upper triangle matrix with real diagonal elements, i.e.,

$$\angle p_{i,i} = 0 \quad p_{\substack{i,j \\ i<j}} = 0 \tag{33}$$

where $p_{i,j}$ is the (i,j)th element of matrix $\mathbf{P}$. Note that the previous constraints on $\mathbf{V}$, given in (33), account for another n^2 real independent constrained equations.

According to the constraints given by (29) and (33), there are total $2k_{\mathrm{c}}(k_{\mathrm{c}} = n^2)$ independent constrained conditions, and the number of free complex dimensions of matrix $\mathbf{V}$ reduces to be $k'_{\mathrm{q}} = tn - n^2$, equivalent to $2k'_{\mathrm{q}}$ free real dimensions. These constrained conditions can be further represented as the following concise manner, which is denoted as a multi-dimensional real function $\mathbf{g}(\mathbf{V})$ given by

$$\mathbf{g}(\mathbf{V}) = \left[\mathbf{g}_1^{\mathsf{T}}(\mathbf{V}), \mathbf{g}_2^{\mathsf{T}}(\mathbf{V}) \right]^{\mathsf{T}} = \mathbf{0},$$
$$\mathbf{g}_i(\mathbf{V}) = [g_{1,1}(\mathbf{V}), g_{1,2}(\mathbf{V}), \dots, g_{1,n^2}(\mathbf{V})]^{\mathsf{T}}, \quad i = 1, 2 \tag{34}$$

where the element functions $g_{i,j}(\cdot)$ of matrices $\mathbf{g}_1(\mathbf{V})$ and $\mathbf{g}_2(\mathbf{V})$ are given by the following form:

$$
\begin{aligned}
g_{1,(i-1)n+i} &= \mathbf{v}_i^{\mathsf{H}}\mathbf{v}_i - 1 \\
g_{2,(i-1)n+i} &= j\left(\mathbf{v}_i^{\mathsf{H}}\hat{\mathbf{v}}_i - \hat{\mathbf{v}}_i^{\mathsf{H}}\mathbf{v}_i \right), \quad 1 \le i \le n \\
g_{1,(i-1)n+k} &= \mathbf{v}_i^{\mathsf{H}}\mathbf{v}_k + \mathbf{v}_k^{\mathsf{H}}\mathbf{v}_i \\
g_{2,(i-1)n+k} &= j\left(\mathbf{v}_i^{\mathsf{H}}\mathbf{v}_k - \mathbf{v}_k^{\mathsf{H}}\mathbf{v}_i \right), \quad 1 \le i < k \le n \\
g_{1,(i-1)n+k} &= \mathbf{v}_i^{\mathsf{H}}\hat{\mathbf{v}}_k + \hat{\mathbf{v}}_k^{\mathsf{H}}\mathbf{v}_i \\
g_{2,(i-1)n+k} &= j\left(\mathbf{v}_i^{\mathsf{H}}\hat{\mathbf{v}}_k - \hat{\mathbf{v}}_k^{\mathsf{H}}\mathbf{v}_i \right), \quad 1 \le k < i \le n
\end{aligned}
\tag{35}
$$

where $\mathbf{v}_i$ and $\hat{\mathbf{v}}_i$ are the ith column of matrices $\mathbf{V} = [\mathbf{v}_1, \dots, \mathbf{v}_n]$ and $\hat{\mathbf{V}} = [\hat{\mathbf{v}}_1, \dots, \hat{\mathbf{v}}_n]$, respectively.

B. High-Resolution Distortion Analysis of Sub-Optimal MIMO CSI Quantizer

According to the second-order Taylor series expansion given by (28) (details provided in Appendix B), distortion function D_{Q} can also be represented by the following form:

$$D_{\mathrm{Q}}(\mathbf{V}, \hat{\mathbf{V}}; \Sigma_{\mathrm{H},n}) = (\mathbf{v} - \hat{\mathbf{v}})^{\mathsf{H}}\mathbf{W}(\hat{\mathbf{V}}; \Sigma_{\mathrm{H},n})(\mathbf{v} - \hat{\mathbf{v}}) \tag{36}$$

where $\mathbf{v} = [\mathbf{v}_1^{\mathsf{T}}, \dots, \mathbf{v}_n^{\mathsf{T}}]^{\mathsf{T}}$, $\hat{\mathbf{v}} = [\hat{\mathbf{v}}_1^{\mathsf{T}}, \dots, \hat{\mathbf{v}}_n^{\mathsf{T}}]^{\mathsf{T}}$, and the (complex) unconstrained sensitivity matrix $\mathbf{W}(\hat{\mathbf{V}}; \Sigma_{\mathrm{H},n})$ is given by

$$\mathbf{W}(\hat{\mathbf{V}}; \Sigma_{\mathrm{H},n}) = \frac{1}{\ln 2}\tilde{\Sigma}_{\mathrm{H},n} \otimes (I - \hat{\mathbf{V}}\hat{\mathbf{V}}^{\mathsf{H}})$$
$$\tilde{\Sigma}_{\mathrm{H},n} = \frac{\rho}{n}\Sigma_{\mathrm{H},n}\left(I + \frac{\rho}{n}\Sigma_{\mathrm{H},n} \right)^{-1}. \tag{37}$$

Moreover, it is also shown in Appendix C that the constrained function $\mathbf{g}(\cdot)$ given by (35) satisfies the necessary and sufficient condition given by (16) (in Proposition 1), thereby leading to a concise distortion analysis in the complex domain. The (complex) constrained sensitivity matrix is hence derived in Appendix C, and has the following form:

$$\mathbf{W}_{\mathrm{c}}(\hat{\mathbf{V}}; \Sigma_{\mathrm{H},n}) = \frac{1}{\ln 2}\tilde{\Sigma}_{\mathrm{H},n} \otimes I_{(t-n)}. \tag{38}$$

By substituting (38) into the complex hyper-ellipsoidal approximation given by (17) (in Proposition 1), the optimal inertial profile is tightly lower bounded by

$$\tilde{I}_{\mathrm{c,opt}}(\hat{\mathbf{V}}; \Sigma_{\mathrm{H},n}) = \frac{(tn - n^2)|\tilde{\Sigma}_{\mathrm{H},n}|^{1/n}}{\ln 2 \cdot (tn - n^2 + 1)\gamma_0^{1/(tn-n^2)}} \tag{39}$$

where γ_0 is a constant given by

$$\gamma_0 = \frac{\pi^{tn-n^2}}{(tn-n^2)!}. \tag{40}$$

It can be observed from (38) and (39) that the constrained sensitivity matrix as well as its corresponding normalized inertial profile are independent of the location $\hat{\mathbf{V}}$.

When the elements of the channel matrix $\mathbf{H}$ are assumed to have i.i.d. complex Gaussian distributions, the matrix $\mathbf{V}$ is independent of the side information $\Sigma_{\mathrm{H},n}$ [36]. Furthermore, $\mathbf{V}$ has a uniform distribution in the complex Stiefel manifold, which is denoted as $\mathcal{V}_{n,t} = \{\mathbf{V} \in \mathbb{C}^{t \times n} : \mathbf{V}^{\mathsf{H}}\mathbf{V} = I_n\}$. Moreover, the probability density function of the orthonormal matrix $\mathbf{V}$ under

constrained condition (35) is derived in Appendix D, and has the following form:

$$p(\mathbf{V}) = \frac{(t-1)\tilde{!}}{\pi^{tn-n^2}(t-n-1)\tilde{!}(n-1)\tilde{!}},$$
$$\text{for } \mathbf{V} \in \mathcal{V}_{n,t} \text{ \& } \mathbf{g}(\mathbf{V}) = \mathbf{0} \quad (41)$$

where we define $k\tilde{!} \triangleq \prod_{i=1}^{k} i!$. Therefore, the average normalized inertial profile of the CSI-quantized MIMO system can be obtained as

$$\tilde{I}_{c,opt}^{w}(\mathbf{V}; \mathbf{\Sigma}_{H,n}) = \frac{(tn-n^2)\beta_1}{\ln 2 \cdot (tn-n^2+1)\gamma_0^{1/(tn-n^2)}} \quad (42)$$

where the constant coefficient β_1 is given by

$$\beta_1 = E[|\tilde{\mathbf{\Sigma}}_{H,n}|^{1/n}] = E\left[\left(\prod_{i=1}^{n} \frac{\rho\lambda_i/n}{1+\rho\lambda_i/n}\right)^{1/n}\right] \quad (43)$$

where $\lambda_1, \ldots, \lambda_n$ are the largest n eigenvalues of matrix $\mathbf{H}^H\mathbf{H}$. Finally, from (11), the asymptotic distortion (or the system capacity loss) of a finite-rate CSI-quantized MIMO system with spatially equal power allocated transmit beamforming scheme is given by

$$C_{Loss} = D \geq \tilde{D}_{Low}$$
$$= \left(\frac{(tn-n^2)\beta_1}{\ln 2 \cdot (tn-n^2+1)}\right.$$
$$\left. \times \left(\frac{(tn-n^2)!(t-n-1)\tilde{!}(n-1)\tilde{!}}{(t-1)\tilde{!}}\right)^{\frac{1}{tn-n^2}}\right)$$
$$\times 2^{-\frac{B}{tn-n^2}}. \quad (44)$$

Moreover, by substituting (41) and (42) into (13), the optimal point density function $\lambda^*(\mathbf{V})$ that achieves the minimal system distortion is a uniform distribution is given by

$$\lambda^*(\mathbf{V}) = \frac{(t-1)\tilde{!}}{\pi^{tn-n^2}(t-n-1)\tilde{!}(n-1)\tilde{!}},$$
$$\text{for } \mathbf{V} \in \mathcal{V}_{n,t} \text{ \& } \mathbf{g}(\mathbf{V}) = \mathbf{0}. \quad (45)$$

C. Interesting Observations of the Distortion Lower Bounds

Based on the expressions of the average distortion lower bound $\tilde{D}_{Low}$ given by (44), the following observations can be made.

1) MIMO systems using maximum ratio transmission (MRT) schemes with finite-rate CSI feedback is a special case of the analysis provided in Section IV-B. In this case, $n = 1$ and $\mathbf{V} \in \mathbb{C}^{t \times 1}$ is the dominant eigenvector of $\mathbf{H}^H\mathbf{H}$. The average system distortion can be lower bounded by

$$\tilde{D}_{Low}^{BF} = \left(\frac{(t-1)\beta_2}{\ln 2 \cdot t}\right) 2^{-\frac{B}{t-1}}, \qquad \beta_2 = E\left[\frac{\rho\lambda_1}{1+\rho\lambda_1}\right] \quad (46)$$

where λ_1 is the largest eigenvalue of matrix $\mathbf{H}^H\mathbf{H}$. By utilizing the statistical properties of the largest eigenvalues of a central Wishart matrix given in [37], coefficient β_2

can be expressed in closed form. Detailed derivations as well as the closed-form analytical results are provided in Appendix E. As a special case of a 2×4 MIMO system with $t = 4, r = 2, \beta_2$ is given by the following form:

$$\beta_2 = \rho\left(12_2F_0(4,1;;-\rho) - 24_2F_0(5,1;;-\rho)\right)$$
$$+ 20_2F_0(6,1;;-\rho)$$
$$- \frac{3}{4}_2F_0\left(4,1;;-\frac{\rho}{2}\right) - \frac{3}{4}_2F_0\left(5,1;;-\frac{\rho}{2}\right)$$
$$- \frac{5}{16}_2F_0\left(6,1;;-\frac{\rho}{2}\right)\right) \quad (47)$$

where $_pF_q(a_1, \ldots, a_p; b_1, \ldots, b_q; x)$ represents the generalized hyper-geometric function [38].

2) MISO system with t transmit antennas and a single receive antenna is another special case, i.e., $r = n = 1$, where the average system distortion reduces to be the following form:

$$\tilde{D}_{Low}^{MISO} = \left(\frac{t-1}{\ln 2}_2F_0(t+1,1;;-\rho)\rho\right) 2^{-\frac{B}{t-1}}. \quad (48)$$

This result is consistent with the analysis provided in [14] and [21].

3) In high-SNR regimes, $\beta_1 \to 1$ and the average system distortion can be represented by

$$\tilde{D}_{Low}^{H-SNR} = \left(\frac{tn-n^2}{\ln 2 \cdot (tn-n^2+1)}\right.$$
$$\left. \times \left(\frac{(tn-n^2)!(t-n-1)\tilde{!}(n-1)\tilde{!}}{(t-1)\tilde{!}}\right)^{\frac{1}{tn-n^2}}\right)$$
$$\times 2^{-\frac{B}{tn-n^2}}. \quad (49)$$

One can observe from (13) that in high-SNR regimes, the average distortion (or system capacity loss) of a $t \times r$ MIMO system using a precoder with n beams (with equal power allocation) is exactly the same as that of the same system using a precoder with $(t-n)$ beams. This means that for a MIMO system with t transmit antennas, quantizing the first n singular vectors of $\mathbf{H}$ (matrix $\mathbf{V}$) is equivalent to quantizing the rest $(t-n)$ singular vectors of $\mathbf{H}$ (matrix $\mathbf{V}^\perp$). In another word, quantizing the orthonormal matrix $\mathbf{V}$ under the constrained condition given by (35) is the same as quantizing the projection matrix $\mathbf{V}\mathbf{V}^H$ (or $\mathbf{V}^\perp\mathbf{V}^{\perp H}$) with $(tn-n^2)$ complex degrees of freedom, which is equivalent to $2(tn-n^2)$ real degrees of freedom.

4) The average system distortion decreases exponentially with a factor of $2^{-B/(tn-n^2)}$, where the exponential component is inversely proportional to the (complex) degrees of freedom of the source variable to be quantized, which is equal to $(tn-n^2)$.

5) For a MIMO system with t transmit antennas, source variable $\mathbf{V}$ (under the constrained condition given by (34) and (35)) has the maximum degrees of freedom when $n = t/2$. It is regarded as the worse-case scenario in terms of having the largest capacity loss. However, it does not necessarily mean $n = t/2$ leads to the smallest system capacity. This

is because $C_{\text{quan}} = C_{\text{perf}} - C_{\text{Loss}}$, and the reference capacities C_{perf} (capacity with ideal quantization of the $\mathbf{V}$ matrix) are different for different number of spatial streams n.

6) When $t = n$ (assuming $r \geq t$), $\mathbf{V}$ is a square unitary matrix. According to capacity loss analysis provided by (44), the total degrees of freedom is *zero*, and hence $C_{\text{Loss}} = 0$. Intuitively speaking, this is because the instantaneous capacity C_{L} is invariant under any unitary rotations on matrix $\mathbf{V}$ at the right hand side. Therefore, all unitary precoding matrices lead to the same instantaneous capacity C_{L}. There is *no* capacity loss due to finite-rate quantization of the precoding matrix.

V. EXTENDED ANALYSIS OF MIMO SYSTEMS WITH FINITE-RATE CSI FEEDBACK

Based on the closed-form analytical results of MIMO systems employing a fixed number of equal power spatial beams obtained in Section IV, two important extensions are provided in this section.

A. Analysis of CSI-Quantizers Using Mismatched High-SNR and Low-SNR Codebooks

Codebook Design Criterions for Transmit Pre-coding Matrices Revisited: In order to obtain an in-depth understanding of MIMO CSI-quantizers using various codebooks, let us recall some codebook design criterions proposed in [14]. First of all, a generalized mean squared weighted inner product (MSwIP) criterion was proposed in the context that it minimizes the system capacity loss. This criterion can be represented by the following form:

$$\max_{\mathcal{C},\mathcal{Q}} E\left[\left\|\hat{\mathbf{V}}^{\mathsf{H}}\mathbf{V}\tilde{\boldsymbol{\Sigma}}_{\mathrm{H},n}^{\frac{1}{2}}\right\|^2\right] \quad \hat{\mathbf{V}} = \mathcal{Q}(\mathbf{H}) \tag{50}$$

where the maximization is w.r.t. to both the codebook $\mathcal{C}$ as well as the encoding algorithm $\mathcal{Q}$. It is not hard to show that the codebook design criterion given by (50) is equivalent to the following criterion:

$$\min_{\mathcal{C},\mathcal{Q}} E[\mathbf{tr}((I - (\mathbf{V}^{\mathsf{H}}\hat{\mathbf{V}})(\mathbf{V}^{\mathsf{H}}\hat{\mathbf{V}})^{\mathsf{H}})\tilde{\boldsymbol{\Sigma}}_{\mathrm{H},n})]$$
$$\hat{\mathbf{V}} = \mathcal{Q}(\mathbf{H}) \tag{51}$$

which is directly related to the distortion function D_{Q} considered in this paper given by (28).

A drawback of the generalized MSwIP design method is that the codebook is optimized for a particular system SNR ρ. Multiple codebooks are needed for MIMO systems operating in an environment with a wide SNR range. Therefore, two alternative codebook design criterions were also proposed in [14], which do not depend on the system SNR. The first design criterion is called high-SNR criterion, where $\rho \to \infty$ and $\tilde{\boldsymbol{\Sigma}}_{\mathrm{H},n} \to I_n$. The optimized high-SNR codebook is designed to maximize the following expectation:

$$\max_{\mathcal{C},\mathcal{Q}} E[\|\hat{\mathbf{V}}^{\mathsf{H}}\mathbf{V}\|^2] \quad \hat{\mathbf{V}} = \mathcal{Q}(\mathbf{H}) \tag{52}$$

which is related to the following high-SNR distortion function

$$D_{\mathrm{Q}}^{\mathrm{H\text{-}snr}}(\mathbf{V}, \hat{\mathbf{V}}) = \frac{1}{\ln 2}\mathbf{tr}(\mathbf{V}^{\mathsf{H}}(I - \hat{\mathbf{V}}\hat{\mathbf{V}}^{\mathsf{H}})\mathbf{V}). \tag{53}$$

Similarly, in the low-SNR regimes, $\rho \to 0$ and $\tilde{\boldsymbol{\Sigma}}_{\mathrm{H},n} \to (\rho/n)\boldsymbol{\Sigma}_{\mathrm{H},n}$. Hence, the low-SNR codebook design criterion is given by

$$\max_{\mathcal{C},\mathcal{Q}} E\left[\left\|\hat{\mathbf{V}}^{\mathsf{H}}\mathbf{V}\boldsymbol{\Sigma}_{\mathrm{H},n}^{\frac{1}{2}}\right\|^2\right] \quad \hat{\mathbf{V}} = \mathcal{Q}(\mathbf{H}) \tag{54}$$

which is related to the following low-SNR distortion function:

$$D_{\mathrm{Q}}^{\mathrm{L\text{-}snr}}(\mathbf{V}, \hat{\mathbf{V}}; \boldsymbol{\Sigma}_{\mathrm{H},n}) = \frac{1}{\ln 2}\mathbf{tr}\left(\mathbf{V}^{\mathsf{H}}(I - \hat{\mathbf{V}}\hat{\mathbf{V}}^{\mathsf{H}})\mathbf{V}\frac{\rho}{n}\boldsymbol{\Sigma}_{\mathrm{H},n}\right). \tag{55}$$

Mismatched Analysis of High-SNR and Low-SNR Codebooks: By utilizing the mismatched analysis described in Section II-F (provided in detail in [25]), we provide in this subsection a distortion (or capacity) analysis of MIMO CSI-quantizers using high-SNR and low-SNR codebooks. First, by the extending the second-order Taylor series expansion results given by (38), the complex constrained sensitivity matrix $\mathbf{W}_{\mathrm{c}}^{\mathrm{H\text{-}snr}}(\mathbf{V}; \boldsymbol{\Sigma}_{\mathrm{H},n})$, which corresponds to distortion function $D_{\mathrm{Q}}^{\mathrm{H\text{-}snr}}$ given by (53), has the following form in high-SNR regimes:

$$\mathbf{W}_{\mathrm{c}}^{\mathrm{H\text{-}snr}}(\mathbf{V}; \boldsymbol{\Sigma}_{\mathrm{H},n}) = \frac{1}{\ln 2}I_{tn-n^2}. \tag{56}$$

By substituting the mismatched (high-SNR) sensitivity matrix (56) into (19), the mismatched inertial profile of the high-SNR codebook can be obtained as

$$\tilde{I}_{\mathrm{mis\text{-}D}}^{\mathrm{H\text{-}snr}}(\mathbf{V}; \tilde{\boldsymbol{\Sigma}}_{\mathrm{H,n}}) = \frac{(tn - n^2)\mathbf{tr}(\tilde{\boldsymbol{\Sigma}}_{\mathrm{H,n}})}{\ln 2 \cdot (tn - n^2 + 1)n\gamma_0^{1/(tn-n^2)}}. \tag{57}$$

Moreover, since the optimal point density given by (45) is a uniform distribution that does not depend on the system SNR, there is no point density mismatch for quantizers using the high SNR codebook. Finally, by substituting (57) and (45) into the distortion integral given by (21), the average system distortion of a MIMO CSI quantizer using high-SNR codebook is given by

$$\tilde{D}_{\mathrm{mis}}^{\mathrm{H\text{-}snr}} = \left(\frac{(tn - n^2)\beta_3}{\ln 2 \cdot (tn - n^2 + 1)}\right.$$
$$\left. \times \left(\frac{(tn - n^2)!(t - n - 1)\tilde{!}(n - 1)\tilde{!}}{(t - 1)\tilde{!}}\right)^{\frac{1}{tn-n^2}}\right)$$
$$\times 2^{-\frac{B}{tn-n^2}} \tag{58}$$

where coefficient β_3 is given by

$$\beta_3 = E\left[\frac{1}{n}\sum_{i=1}^{n}\frac{\rho\lambda_i/n}{1 + \rho\lambda_i/n}\right]. \tag{59}$$

By utilizing similar derivations, the low-SNR constrained sensitivity matrix can also be obtained

$$\mathbf{W}_c^{\text{L-snr}}(\mathbf{V}; \boldsymbol{\Sigma}_{\text{H},n}) = \frac{\rho}{\ln 2 \cdot n} \boldsymbol{\Sigma}_{\text{H},n} \otimes I_{t-n} \qquad (60)$$

which leads to the following mismatched inertial profile:

$$\tilde{I}_{\text{mis-D}}^{\text{L-snr}}(\mathbf{V}; \tilde{\boldsymbol{\Sigma}}_{\text{H},n})$$
$$= \frac{(tn - n^2) \left| \frac{\rho}{n} \boldsymbol{\Sigma}_{\text{H},n} \right|^{1/n} \mathbf{tr} \left(I + \frac{\rho}{n} \boldsymbol{\Sigma}_{\text{H},n} \right)^{-1}}{\ln 2 \cdot (tn - n^2 + 1) n \gamma_0^{1/(tn-n^2)}}. \qquad (61)$$

Once again, by substituting (61) and (45) into the distortion integral (21), the average system distortion of a MIMO CSI quantizer using low-SNR codebook is given by

$$\tilde{D}_{\text{mis}}^{\text{L-snr}} = \left(\frac{(tn - n^2)\beta_4}{\ln 2 \cdot (tn - n^2 + 1)} \right.$$
$$\left. \times \left(\frac{(tn - n^2)!(t - n - 1)\tilde{!}(n - 1)\tilde{!}}{(t - 1)\tilde{!}} \right)^{\frac{1}{tn-n^2}} \right)$$
$$\times 2^{-\frac{B}{tn-n^2}} \qquad (62)$$

where coefficient β_4 is given by

$$\beta_4 = E \left[\left(\prod_{i=1}^{n} \frac{\rho}{n} \lambda_i \right)^{1/n} \left(\frac{1}{n} \sum_{i=1}^{n} \frac{1}{1 + \rho\lambda_i/n} \right) \right]. \qquad (63)$$

As a direct results of the previous mismatched analysis, MIMO CSI-quantizers using mismatched high-SNR and low-SNR codebooks give rise to the following performance losses:

$$L_{\text{H-snr}} = \frac{\tilde{D}_{\text{mis}}^{\text{H-snr}}}{\tilde{D}_{\text{Low}}} = \frac{\beta_3}{\beta_1} \quad L_{\text{L-snr}} = \frac{\tilde{D}_{\text{mis}}^{\text{L-snr}}}{\tilde{D}_{\text{Low}}} = \frac{\beta_4}{\beta_1}. \qquad (64)$$

The performance losses $L_{\text{H-snr}}$ and $L_{\text{L-snr}}$ defined in (64) can be viewed as a capacity penalty for using the mismatched high-SNR and low-SNR codebooks instead of the optimal codebook designed to match a specific SNR point. Both losses can be shown to be greater than one, i.e., $L_{\text{H-snr}}, L_{\text{L-snr}} \geq 1$, and are independent of the quantization resolution (feedback rate) B, which is shown by (64).

B. Analysis of MIMO Precoding Schemes With Multi-Mode Spatial Multiplexing Strategy

In order to compensate for the loss due to the equal power allocation among the spatial beams used by the transmit precoder, a multi-mode spatial multiplexing (MMSM) scheme was proposed in [14], where the number of active spatial beams employed by the transmitter is adjusted adaptively accordingly to the current system SNR. As an example, we plot in Fig. 1 the normalized capacity of a 4×3 MIMO system ($t = 4, r = 3$) over i.i.d. fading channels with finite-rate CSI feedback of $B = 8$ bits per channel update. The normalized MIMO capacity is
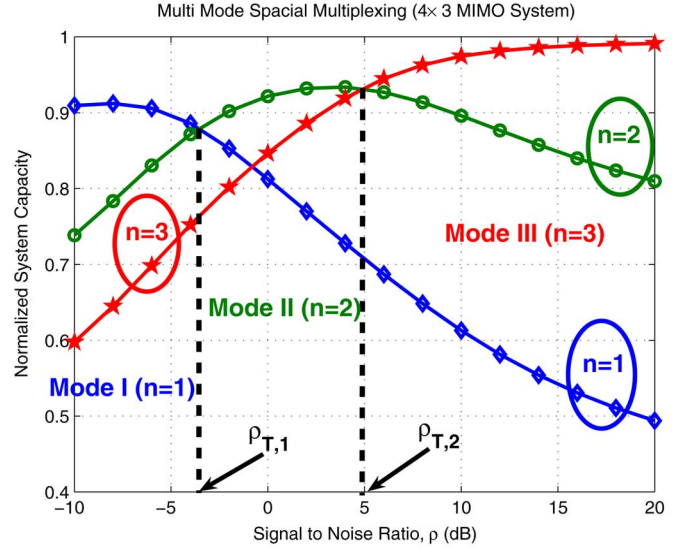

Fig. 1. Normalized system capacity of a 4×3 MIMO system ($t = 4, r = 3$) over i.i.d. Rayleigh fading channels with finite-rate CSI feedback ($B = 8$), and using multi-mode spatial multiplexing transmission schemes.

defined to be the ratio of the system capacity with quantized CSI to that of a system using optimal transmit precoder with ideal CSIT. The proposed multi-mode transmission strategy is employed for the system simulation, where the MIMO transmit precoder used for each mode has n active spatial beams with equal power allocation. For this particular case, there are total $\min(t, r) = 3$ modes available for the current MIMO system, i.e., $1 \leq n \leq 3$. The codebooks of the CSI quantizer used at each mode are generated by the generalized mean-squared weighted inner-product (MSwIP) criterion proposed in [14]. It can be observed from Fig. 1 that by switching the modes based on the SNR, one can use the best mode and the system capacity of using the MMSM scheme is the maximum of the capacity of all the available modes.

As a direct result of the high-rate analysis obtained in Section V-A, the system capacity of a $t \times r$ MIMO system with finite-rate CSI feedback of B bits per channel update, and using MMSM transmission scheme with high-SNR codebooks can be represented by the following form:

$$C_{\text{MMSM}} =$$
$$\max_{1 \leq n \leq \min(t,r)} \left(E \left[\sum_{i=1}^{n} \log_2 \left(1 + \frac{\rho}{n} \lambda_i \right) \right] - \alpha_n 2^{-\frac{B}{tn-n^2}} \right) \qquad (65)$$

where α_n is a coefficient that depends on t, r, n and ρ, which is given by

$$\alpha_n(\rho) = \frac{(tn - n^2)\beta_3}{\ln 2 \cdot (tn - n^2 + 1)}$$
$$\times \left(\frac{(tn - n^2)!(t - n - 1)\tilde{!}(n - 1)\tilde{!}}{(t - 1)\tilde{!}} \right)^{\frac{1}{tn-n^2}} \qquad (66)$$

with β_3 given by (59). Consequently, for a particular operating SNR of the system, which is assumed to change at a much
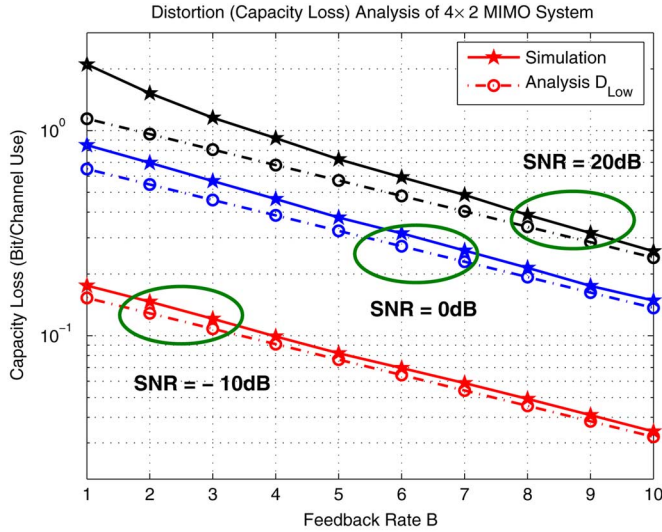
Fig. 2. Capacity loss versus CSI feedback rate B of a 4×2 MIMO system ($t = 4, r = 2$, and $n = 2$) over i.i.d. Rayleigh fading channels and with SNR $\rho = -10, 0$, and 20 dB.

Fig. 3. Performance losses ($L_{\text{H-snr}}$ and $L_{\text{L-snr}}$) versus SNR ρ of a 4×3 MIMO system ($t = 4, r = 3$, and $n = 2$) over i.i.d. Rayleigh fading channels with feedback rate $B = 8$ bits per channel update.

slower rate than the channel itself, the best transmission mode is given by

$$n_{\text{opt}} =$$

$$\arg \max_{1 \leq n \leq \min(t,r)} \left(E\left[\sum_{i=1}^{n} \log_2 \left(1 + \frac{\rho}{n} \lambda_i \right) \right] - \alpha_n 2^{-\frac{B}{tn - n^2}} \right).$$

$$(67)$$

Based on the analytical result of the MMSM precoder given by (65) and (67), the boundary points of the mode transitions (such as $\rho_{T,1}$ and $\rho_{T,2}$ in Fig. 1) can be calculated analytically without actual simulations.

VI. NUMERICAL AND SIMULATION RESULTS

A. High-Rate Capacity Analysis

Some numerical experiments are now presented to provide a better feel for the utility of the distortion analysis. Fig. 2 shows the capacity loss due to the finite-rate quantization of the CSI versus feedback rate B for a 4×2 MIMO system ($t = 4, r = 2$) over i.i.d. Rayleigh flat fading channels under different system SNRs at $\rho = -10, 0$, and 20 dB, respectively. The transmit precoder used for the MIMO system has $n = 2$ spatial beams with equal power allocations. The codebook of the CSI quantizer is generated by using the generalized mean-squared weighted inner-product (MSwIP) criterion [14]. The distortion lower bounds $\tilde{D}_{\text{Low}}$ given by (44) are also included in the plot for comparisons. It can be observed from the plot that the proposed distortion (or system capacity loss) lower bounds are tight and predict very well the actual system capacity loss obtained from Monte Carlo simulations.

B. Analysis of Mismatched High-SNR and Low-SNR Codebooks

In order to understand the performance degradation caused by the mismatched CSI-quantizers using high-SNR and low-SNR
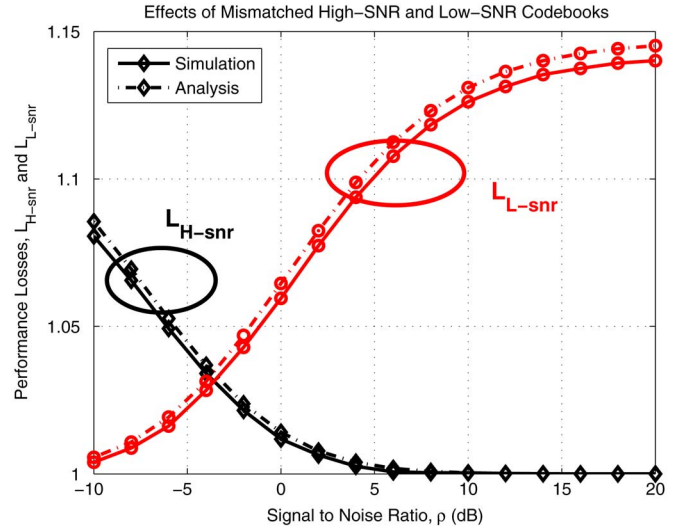
codebooks, we plot in Fig. 3 the performance losses $L_{\text{H-snr}}$ and $L_{\text{L-snr}}$ versus the system SNR ρ of a 4×3 MIMO system ($t = 4, r = 3$) with finite-rate CSI feedback of $B = 8$ bits per channel update. The performance losses $L_{\text{H-snr}}$ and $L_{\text{L-snr}}$ represent the ratio of the average system distortion of a mismatched quantizer to that of the optimal quantizer, whose definition is given by (64). The transmit precoder used for the MIMO system has $n = 2$ spatial beams with equal power allocations. The codebook of the CSI quantizer is also generated by using the generalized MSwIP criterion. For comparison purpose, the ratios of the distortion bounds, i.e., $\tilde{D}_{\text{mis}}^{\text{H-snr}}/\tilde{D}_{\text{Low}}$ and $\tilde{D}_{\text{mis}}^{\text{L-snr}}/\tilde{D}_{\text{Low}}$, are also included in the plot. It can be observed from Fig. 3 that the obtained performance losses (or system distortion ratios) agree well with the simulation results.

C. Performance of Multi-Mode Spatial Multiplexing Schemes

In order to see the utility of the proposed distortion analysis to MIMO systems using multi-mode spatial multiplexing transmission schemes, we demonstrate in Fig. 4 the normalized capacity of the same 4×3 MIMO system ($t = 4, r = 3$), which is described in Section V-B, over i.i.d. Rayleigh fading channels with CSI feedback of $B = 8$ bits per channel update. The MIMO precoder again employs the MMSM scheme, with total three modes available ($n = 1, 2, 3$). Both the capacity analysis given by (65) as well as the results obtained from Monte Carlo simulations are shown in Fig. 4. It can be observed from the plot that the proposed capacity analysis closely matches the simulation results.

We also demonstrate in Fig. 5, the analytical results of the normalized system capacity of the same 4×3 MIMO system ($t = 4, r = 3$) using MMSM transmission schemes but with different rate of CSI feedback of $B = 1, 3, 5, 8$ bits per channel update. For the sake of comparison, we also include in the plot the normalized capacity of MIMO system with no CSI feedback, which corresponds to the case where no CSIT is available and the MIMO transmitter sends independent data stream on each of its antennas with equal power allocations. It can be observed
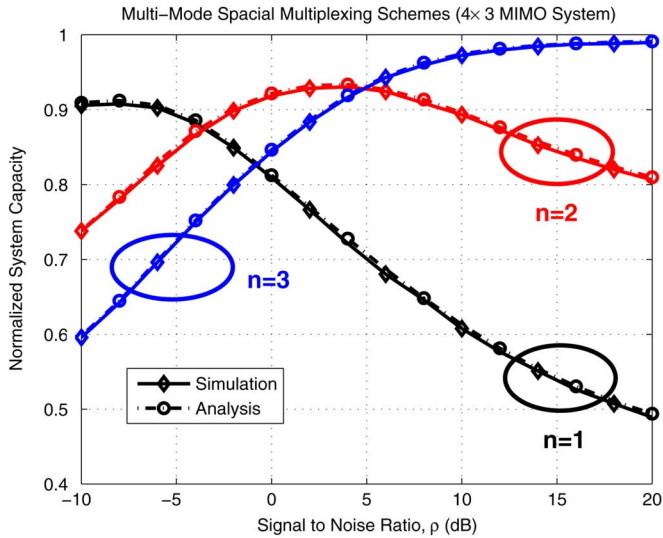
Fig. 4. Normalized system capacity of a 4×3 MIMO system ($t = 4$, $r = 3$) over i.i.d. Rayleigh fading channels with feedback rate $B = 8$ bits per channel update and using multi-mode spatial multiplexing (MMSM) transmission schemes.
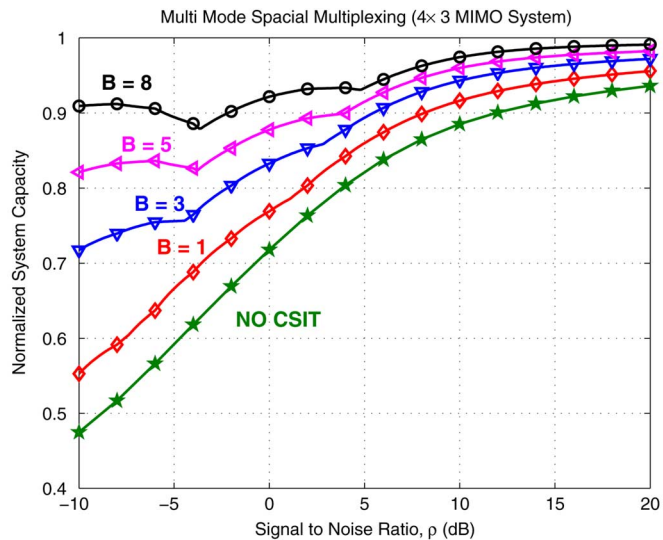

Fig. 5. Normalized system capacity of a 4×3 MIMO system ($t = 4$, $r = 3$) over i.i.d. Rayleigh fading channels using MMSM transmission scheme, and with several different CSI feedback rate ($B = 1, 3, 5, 8$ bits per channel update).

from Fig. 5 that the system capacity improves significantly as the feedback rate B increases. To be specific, we can see that with a feedback rate of $B = 8$ bits, a 4×3 MIMO system with MMSM scheme can almost achieve 90% of the capacity of a system with ideal CSIT. Compared with the total free dimensions of the original CSI information $\mathbf{H}$, which is 24, only 1/3 bits per dimension is needed for a properly designed MIMO CSI feedback scheme. This is very encouraging as the results suggest that in order to achieve a performance in terms of capacity close to that of systems with ideal CSIT, only limited CSI feedback rate per dimension is required.

VII. CONCLUSION

This paper analyzes the behavior of MIMO systems with limited feedback precoding matrices using high resolution quantization theory. To enhance the tractability of the analysis, the distortion analysis of vector quantizers was first extended to deal with complex source variables such that it is directly applicable in the complex domain without having to first transform into real vectors. This is especially important for source variables with large dimensions (i.e., MIMO systems with finite-rate CSI feedback) because the analysis is more cumbersome if performed in the real domain. Necessary and sufficient conditions that guarantee a concise high-resolution distortion analysis in the complex domain were also presented. The proposed complex distortion analysis was then used to provide tight lower bounds on the capacity loss of MIMO systems due to the finite-rate quantization of the transmit precoding matrices. In addition, exploiting the generality of high-resolution quantization framework, MIMO CSI-quantizers with mismatched codebooks that are only optimized for high-SNR and low-SNR regimes were also analyzed to quantify the penalties caused by the mismatched codebooks. Capacity analysis of MIMO systems using multi-mode spatial multiplexing schemes with finite-rate CSI feedback was also provided. Numerical and simulation results were provided which confirm the tightness of theoretical distortion bounds.

APPENDIX A
PROOF OF PROPOSITION 1

Proof: (Sufficient Condition:) According to the property of the complex derivative provided in [32], the following equality is valid:

$$\frac{\partial \mathbf{g}(\bar{\mathbf{y}})}{\partial \bar{\mathbf{y}}} = \frac{\partial \mathbf{g}(\tilde{\mathbf{y}})}{\partial \tilde{\mathbf{y}}} \begin{bmatrix} I_{k_{\mathrm{q}}} & j I_{k_{\mathrm{q}}} \\ I_{k_{\mathrm{q}}} & -j I_{k_{\mathrm{q}}} \end{bmatrix}$$
$$\bar{\mathbf{y}} = \left[\mathbf{y}_{\mathrm{R}}^{\mathsf{T}}, \mathbf{y}_{\mathrm{I}}^{\mathsf{T}} \right]^{\mathsf{T}}$$
$$\bar{\mathbf{y}}' = \left[-\mathbf{y}_{\mathrm{I}}^{\mathsf{T}}, \mathbf{y}_{\mathrm{R}}^{\mathsf{T}} \right]^{\mathsf{T}} \tag{68}$$

where $\mathbf{y}_{\mathrm{R}}$ and $\mathbf{y}_{\mathrm{I}}$ are the real and imaginary part of $\mathbf{y}$. By substituting (16) into (68) and after some manipulations, we can obtain the following relation:[9]

$$\overline{\frac{\partial \mathbf{g}_1(\mathbf{y})}{\partial \mathbf{y}}} = \begin{bmatrix} I_{k_{\mathrm{c}}} & \mathbf{0} \\ \mathbf{0} & j\mathbf{\Phi} \end{bmatrix} \frac{\partial \mathbf{g}(\bar{\mathbf{y}})}{\partial \bar{\mathbf{y}}}. \tag{69}$$

Since the column vectors of matrix $\mathbf{V}_2 \in \mathbb{C}^{k_{\mathrm{q}} \times k'_{\mathrm{q}}}$ span the null space $\mathcal{N}(\partial/\partial \mathbf{y} \mathbf{g}_1(\mathbf{y}))$, it is evident that column vectors of $\overline{\mathbf{V}}_2$ should span the null space of $\mathcal{N}(\overline{(\partial/\partial \mathbf{y}) \mathbf{g}_1(\mathbf{y})})$. Moreover, according to (69), columns of matrix $\bar{\mathbf{V}}_2$ also span the null space $\mathcal{N}((\partial/\partial \bar{\mathbf{y}}) \mathbf{g}(\bar{\mathbf{y}}))$. By employing the same reasoning used in

[9]Operation $\overline{\mathbf{A}}$ of a matrix $\mathbf{A}$ is defined to be

$$\bar{\mathbf{A}} = \begin{bmatrix} \mathbf{A}_{\mathrm{R}} & \mathbf{A}_{\mathrm{I}} \\ -\mathbf{A}_{\mathrm{I}} & \mathbf{A}_{\mathrm{R}} \end{bmatrix}$$

where $\mathbf{A}_{\mathrm{R}}$ and $\mathbf{A}_{\mathrm{I}}$ represents the real and imaginary part of matrix $\mathbf{A}$.

[21], one can obtain the following second-order Taylor series expansion of the distortion function after some manipulations:

$$D_Q(\mathbf{y}, \hat{\mathbf{y}}; \mathbf{z}) \approx \overline{(\mathbf{y} - \hat{\mathbf{y}})}^\mathsf{T} \bar{\mathbf{V}}_2 \bar{\mathbf{V}}_2^\mathsf{T} \overline{\mathbf{W}_{c,z}(\hat{\mathbf{y}})} \bar{\mathbf{V}}_2 \overline{\mathbf{V}}_2^\mathsf{T} \overline{(\mathbf{y} - \hat{\mathbf{y}})}$$
$$= \mathbf{e}^\mathsf{H} \mathbf{W}_{c,z}(\hat{\mathbf{y}}) \mathbf{e} \tag{70}$$

where vector $\mathbf{e} \in \mathbb{C}^{k_q'} \times 1$ is given by $\mathbf{e} = \mathbf{V}_2^\mathsf{H}(\mathbf{y} - \hat{\mathbf{y}})$. Again, by extending the same reasonings used in the analysis of real vectors, the constrained complex inertial profile (14) as well as its tight lower bound (17) can be obtained.

(Necessary Condition:) On the other hand, if the distortion function D_Q has a concise second-order approximation given by (70), which can further lead to a concise inertial profile expression, the column vectors of matrix $\bar{\mathbf{V}}_2$ span the null space $\mathcal{N}((\partial/\partial \bar{\mathbf{y}}) \mathbf{g}(\bar{\mathbf{y}}))$. This means that the two range spaces $\mathcal{R}(((\partial/\partial \bar{\mathbf{y}}) \mathbf{g}(\bar{\mathbf{y}}))^\mathsf{T})$ and $\mathcal{R}(((\partial/\partial \mathbf{y}) \mathbf{g}_1(\mathbf{y}))^\mathsf{T})$ are equivalent. Moreover, it can be shown that the following equality is valid:

$$\mathcal{R}\left(\left(\overline{\frac{\partial \mathbf{g}_1(\mathbf{y})}{\partial \mathbf{y}}}\right)^\mathsf{T}\right) = \mathcal{R}\left(\left[\frac{\partial \mathbf{g}_1(\bar{\mathbf{y}})}{\partial \bar{\mathbf{y}}}^\mathsf{T}, \frac{\partial \mathbf{g}_1(\bar{\mathbf{y}}')}{\partial \bar{\mathbf{y}}'}^\mathsf{T}\right]\right)$$
$$= \mathcal{R}\left(\frac{\partial \mathbf{g}_1(\bar{\mathbf{y}})}{\partial \bar{\mathbf{y}}}^\mathsf{T}\right) \oplus \mathcal{R}\left(\frac{\partial \mathbf{g}_1(\bar{\mathbf{y}}')}{\partial \bar{\mathbf{y}}'}^\mathsf{T}\right) \tag{71}$$

where "$\oplus$" represents the subspace summation. Similarly, one can also obtain the following equality:

$$\mathcal{R}\left(\left(\frac{\partial \mathbf{g}(\bar{\mathbf{y}})}{\partial \bar{\mathbf{y}}}\right)^\mathsf{T}\right) = \mathcal{R}\left(\left[\frac{\partial \mathbf{g}_1(\bar{\mathbf{y}})}{\partial \bar{\mathbf{y}}}^\mathsf{T}, \frac{\partial \mathbf{g}_2(\bar{\mathbf{y}})}{\partial \bar{\mathbf{y}}}^\mathsf{T}\right]\right)$$
$$= \mathcal{R}\left(\frac{\partial \mathbf{g}_1(\bar{\mathbf{y}})}{\partial \bar{\mathbf{y}}}^\mathsf{T}\right) \oplus \mathcal{R}\left(\frac{\partial \mathbf{g}_2(\bar{\mathbf{y}})}{\partial \bar{\mathbf{y}}}^\mathsf{T}\right). \tag{72}$$

It is evident from (71) and (72) that the two range spaces $\mathcal{R}(((\partial/\partial \bar{\mathbf{y}}') \mathbf{g}_1(\bar{\mathbf{y}}'))^\mathsf{T})$ and $\mathcal{R}(((\partial/\partial \bar{\mathbf{y}}) \mathbf{g}_2(\bar{\mathbf{y}}))^\mathsf{T})$ are equivalent and there exists a non-singular matrix $\mathbf{\Psi}$ such that

$$\frac{\partial \mathbf{g}_1(\bar{\mathbf{y}}')}{\partial \bar{\mathbf{y}}'} = \mathbf{\Psi} \frac{\partial \mathbf{g}_2(\bar{\mathbf{y}})}{\partial \bar{\mathbf{y}}}. \tag{73}$$

From (73), one can further obtain the following equality after some manipulations:

$$\frac{\partial \mathbf{g}_1(\tilde{\mathbf{y}}')}{\partial \tilde{\mathbf{y}}'} = \left(\frac{-j\mathbf{\Psi}}{2}\right) \frac{\partial \mathbf{g}_2(\tilde{\mathbf{y}})}{\partial \tilde{\mathbf{y}}}. \tag{74}$$

Therefore, as long as the rows of two derivatives matrices $(\partial \mathbf{g}_1(\tilde{\mathbf{y}}')/\partial \tilde{\mathbf{y}}')$ and $(\partial \mathbf{g}_2(\tilde{\mathbf{y}})/\partial \tilde{\mathbf{y}})$ span the same subspace, the complex constrained inertial profile can be expressed in a concise form.

APPENDIX B
SECOND ORDER TAYLOR SERIES EXPANSION OF THE DISTORTION FUNCTION D_Q

It is noted that the distortion function D_Q (or the instantaneous capacity loss C_L) given by (27) is a real-valued function of complex variable $\mathbf{V}_H$. We therefore utilize the Wirtinger calculous [31] to obtain the complex derivative and complex Hessian matrix of the distortion function with respect to $\mathbf{V}_H$.

Let us first consider a real-valued complex function $f(\mathbf{X})$ given by the following form:

$$f(\mathbf{X}; \mathbf{A}_1, \mathbf{A}_2) = \log_2 \det\left(I + \mathbf{A}_1 \mathbf{X}^\mathsf{H} \mathbf{A}_2 \mathbf{X}\right) \tag{75}$$

where $\mathbf{A}_1$ and $\mathbf{A}_2$ are semi-definite complex Hessian matrices. According to the definitions given in [32], the generalized complex derivative of function $f(\mathbf{X})$ can be obtained by the following form:

$$\mathbf{d}_f = \left[\frac{\partial}{\partial \mathbf{x}^\star} f(\mathbf{X})\right]^\mathsf{T}$$
$$= \frac{1}{\ln 2} \mathrm{vec}(\mathbf{A}_2 \mathbf{X}(I + \mathbf{A}_1 \mathbf{X}^\mathsf{H} \mathbf{A}_2 \mathbf{X})^{-1} \mathbf{A}_1) \tag{76}$$

where $\mathbf{x} = \mathrm{vec}(\mathbf{X})$. Furthermore, the complex Hessian matrices of $f(\mathbf{X})$ can also be obtained as

$$\mathbf{\Phi}_f = \frac{\partial \mathbf{d}_f}{\partial \mathbf{x}}$$
$$= \frac{1}{\ln 2} \left(\mathbf{A}_1^\mathsf{T}(I + \mathbf{A}_1 \mathbf{X}^\mathsf{H} \mathbf{A}_2 \mathbf{X})^{-\mathsf{T}}\right)$$
$$\otimes \left(\mathbf{A}_2 - \mathbf{A}_2 \mathbf{X}(I + \mathbf{A}_1 \mathbf{X}^\mathsf{H} \mathbf{A}_2 \mathbf{X})^{-1} \mathbf{A}_1 \mathbf{X}^\mathsf{H} \mathbf{A}_2\right) \tag{77}$$
$$\mathbf{\Phi}_f' = \frac{\partial \mathbf{d}_f}{\partial \mathbf{x}^\star}$$
$$= \frac{-1}{\ln 2} \left(\left(\mathbf{A}_1^\mathsf{T}(I + \mathbf{A}_1 \mathbf{X}^\mathsf{H} \mathbf{A}_2 \mathbf{X})^{-\mathsf{T}} \mathbf{X}^\mathsf{T} \mathbf{A}_2^\mathsf{T}\right)\right.$$
$$\left.\otimes \left(\mathbf{A}_2 \mathbf{X}(I + \mathbf{A}_1 \mathbf{X}^\mathsf{H} \mathbf{A}_2 \mathbf{X})^{-1} \mathbf{A}_1\right)\right) \mathbf{P} \tag{78}$$

where $\mathbf{P}$ (of size $tn \times tn$) is a permutation matrix defined as

$$\mathbf{P} = \sum_{r=1}^{t} \sum_{s=1}^{n} \mathbf{E}_{rs} \otimes \mathbf{E}_{sr} \tag{79}$$

where $\mathbf{E}_{rs}$ (of size $t \times n$) and $\mathbf{E}_{sr}$ (of size $n \times t$) are elementary matrices which have unity in the $(r, s)^{\text{th}}$ or $(s, r)^{\text{th}}$ position and all other elements are zero.

The distortion function D_Q (or the instantaneous capacity loss C_L) given by (27) can also be represented as the following form:

$$D_Q = C_L = f\left(\mathbf{V}_H; \begin{bmatrix} \frac{\rho}{n} \mathbf{\Sigma}_{H,n} & \mathbf{0} \\ \mathbf{0} & \mathbf{0} \end{bmatrix}, I_t\right)$$
$$- f\left(\mathbf{V}_H; \frac{\rho}{n} \mathbf{\Sigma}_H, \hat{\mathbf{V}} \hat{\mathbf{V}}^\mathsf{H}\right). \tag{80}$$

After some manipulations, the complex derivative of function D_Q can be obtained

$$\mathbf{d}_Q = \left[\frac{\partial}{\partial \mathbf{v}_H^\star} D_Q(\mathbf{V}_H)\right]^\mathsf{T}\bigg|_{\mathbf{V}_H = \hat{\mathbf{V}}_H}$$
$$= \mathbf{0}$$
$$\hat{\mathbf{V}}_H = [\hat{\mathbf{V}}, \mathbf{V}']$$
$$\mathbf{v}_H^\star = \mathrm{vec}(\mathbf{V}_H). \tag{81}$$

Moreover, according to (77) and (78), the Hessian matrices of D_{Q} can also be obtained as

$$
\begin{aligned}
\boldsymbol{\Phi}_{\mathrm{Q}} &= \left.\frac{\partial \mathbf{d}_{\mathrm{Q}}}{\partial \mathbf{v}_{\mathrm{H}}}\right|_{\mathbf{V}_{\mathrm{H}}=\hat{\mathbf{V}}_{\mathrm{H}}} \\
&= \frac{1}{\ln 2}\begin{bmatrix} \tilde{\boldsymbol{\Sigma}}_{\mathrm{H},n} & \mathbf{0} \\ \mathbf{0} & \mathbf{0} \end{bmatrix} \otimes (I - \hat{\mathbf{V}}\hat{\mathbf{V}}^{\mathsf{H}}) \\
\boldsymbol{\Phi}'_{\mathrm{Q}} &= \left.\frac{\partial \mathbf{d}_{\mathrm{Q}}}{\partial \mathbf{v}_{\mathrm{H}}^{\star}}\right|_{\mathbf{V}_{\mathrm{H}}=\hat{\mathbf{V}}_{\mathrm{H}}} \\
&= \mathbf{0} \qquad\qquad\qquad\qquad\qquad (82)
\end{aligned}
$$

where matrix $\tilde{\boldsymbol{\Sigma}}_{\mathrm{H},n}$ is given by

$$
\tilde{\boldsymbol{\Sigma}}_{\mathrm{H},n} = \frac{\rho}{n}\boldsymbol{\Sigma}_{\mathrm{H},n}\left(I + \frac{\rho}{n}\boldsymbol{\Sigma}_{\mathrm{H},n}\right)^{-1}. \qquad (83)
$$

It is shown in [32] that a real-valued complex function has the following second-order Taylor series expansion:

$$
\begin{aligned}
D_{\mathrm{Q}}(\mathbf{V}_{\mathrm{H}}) =\ & D_{\mathrm{Q}}(\hat{\mathbf{V}}_{\mathrm{H}}) + 2\Re[(\mathbf{v}_{\mathrm{H}} - \hat{\mathbf{v}}_{\mathrm{H}})^{\mathsf{H}}\mathbf{d}_{\mathrm{Q}}] \\
& + \Re[(\mathbf{v}_{\mathrm{H}} - \hat{\mathbf{v}}_{\mathrm{H}})^{\mathsf{H}}\boldsymbol{\Phi}_{\mathrm{Q}}(\mathbf{v}_{\mathrm{H}} - \hat{\mathbf{v}}_{\mathrm{H}}) \\
& + (\mathbf{v}_{\mathrm{H}} - \hat{\mathbf{v}}_{\mathrm{H}})\boldsymbol{\Phi}'_{\mathrm{Q}}(\mathbf{v}_{\mathrm{H}} - \hat{\mathbf{v}}_{\mathrm{H}})^{\star}] + \text{h.o.t} \quad (84)
\end{aligned}
$$

where vector $\hat{\mathbf{v}}_{\mathrm{H}} = \mathbf{vec}(\hat{\mathbf{V}}_{\mathrm{H}})$ and "h.o.t." stands for higher order terms. By substituting (81) and (82) into the Taylor series expansion given by (84), one can obtain the following result:

$$
\begin{aligned}
D_{\mathrm{Q}} \approx\ & \frac{1}{\ln 2}(\mathbf{v}_{\mathrm{H}} - \hat{\mathbf{v}}_{\mathrm{H}})^{\mathsf{H}}\left(\begin{bmatrix} \tilde{\boldsymbol{\Sigma}}_{\mathrm{H},n} & \mathbf{0} \\ \mathbf{0} & \mathbf{0} \end{bmatrix} \otimes (I - \hat{\mathbf{V}}\hat{\mathbf{V}}^{\mathsf{H}})\right) \\
& \times (\mathbf{v}_{\mathrm{H}} - \hat{\mathbf{v}}_{\mathrm{H}}) \\
=\ & \frac{1}{\ln 2}\mathbf{tr}((\mathbf{V} - \hat{\mathbf{V}})^{\mathsf{H}}(I - \hat{\mathbf{V}}\hat{\mathbf{V}}^{\mathsf{H}})(\mathbf{V} - \hat{\mathbf{V}})\tilde{\boldsymbol{\Sigma}}_{\mathrm{H},n}) \\
=\ & \frac{1}{\ln 2}(\mathbf{v} - \hat{\mathbf{v}})^{\mathsf{H}}(\tilde{\boldsymbol{\Sigma}}_{\mathrm{H},n} \otimes (I - \hat{\mathbf{V}}\hat{\mathbf{V}}^{\mathsf{H}}))(\mathbf{v} - \hat{\mathbf{v}}). \quad (85)
\end{aligned}
$$

It can be observed from (85) that D_{Q} (up to the second-order approximation) is a function of $\mathbf{V}$ and $\hat{\mathbf{V}}$, parameterized only by $\boldsymbol{\Sigma}_{\mathrm{H},n}$.

APPENDIX C
DERIVATIVE OF THE CONSTRAINED SENSITIVITY MATRIX $\mathbf{W}_{\mathrm{c}}(\hat{\mathbf{V}}; \boldsymbol{\Sigma}_{\mathrm{H},n})$

First of all, it is clear that $\mathbf{g}(\cdot)$ given in (35) is a multi-dimensional real function of size $2n^2 \times 1$. According to the method of Wirtinger calculus [32], we can first obtain the following partial derivative of function $\mathbf{g}(\cdot)$ w.r.t. vector $\mathbf{v}^*$:

$$
\left.\frac{\partial}{\partial \mathbf{v}^*}\mathbf{g}_1(\mathbf{V})\right|_{\mathbf{V}=\hat{\mathbf{V}}} = (I + \mathbf{P})(I_n \otimes \hat{\mathbf{V}}^{\mathsf{T}}) \qquad (86)
$$

$$
\left.\frac{\partial}{\partial \mathbf{v}^*}\mathbf{g}_2(\mathbf{V})\right|_{\mathbf{V}=\hat{\mathbf{V}}} = j(I - \mathbf{P})(I_n \otimes \hat{\mathbf{V}}^{\mathsf{T}}) \qquad (87)
$$

where $\mathbf{P} \in \mathbb{R}^{n^2 \times n^2}$ is a sparse matrix with its elements given by

$$
p_{(i-1)n+k,m} = \begin{cases} 1, & \text{for } m = (k-1)n+i \ \& \ i < k \\ 0, & \text{otherwise} \end{cases} \qquad (88)
$$

where $1 \le i, k \le n$ and $1 \le m \le n^2$. After some manipulations, the partial derivative of $\mathbf{g}(\cdot)$ w.r.t. vector $\mathbf{v}$ can also be obtained, which is given by

$$
\left.\frac{\partial}{\partial \mathbf{v}}\mathbf{g}_1(\mathbf{V})\right|_{\mathbf{V}=\hat{\mathbf{V}}} = (I + \mathbf{P})(I_n \otimes \hat{\mathbf{V}}^{\mathsf{H}}) \qquad (89)
$$

$$
\left.\frac{\partial}{\partial \mathbf{v}}\mathbf{g}_2(\mathbf{V})\right|_{\mathbf{V}=\hat{\mathbf{V}}} = -j(I - \mathbf{P})(I_n \otimes \hat{\mathbf{V}}^{\mathsf{H}}). \qquad (90)
$$

Therefore, by defining $\tilde{\mathbf{v}} = [\mathbf{v}^{\mathsf{T}}, \mathbf{v}^{\mathsf{H}}]^{\mathsf{T}}$ and $\tilde{\mathbf{v}}' = [-\mathbf{v}^{\mathsf{T}}, \mathbf{v}^{\mathsf{H}}]^{\mathsf{T}}$, the partial derivatives of function $\mathbf{g}(\cdot)$ w.r.t. vectors $\hat{\mathbf{v}}$ and $\hat{\mathbf{v}}'$ can be obtained as the following form:

$$
\left.\frac{\partial}{\partial \tilde{\mathbf{v}}}\mathbf{g}_1(\mathbf{V})\right|_{\mathbf{V}=\hat{\mathbf{v}}} = (I + \mathbf{P})[-(I_n \otimes \hat{\mathbf{V}}^{\mathsf{H}})\,|\,(I_n \otimes \hat{\mathbf{V}}^{\mathsf{T}})] \quad (91)
$$

$$
\left.\frac{\partial}{\partial \tilde{\mathbf{v}}}\mathbf{g}_2(\mathbf{V})\right|_{\mathbf{V}=\hat{\mathbf{v}}} = j(I - \mathbf{P})[-(I_n \otimes \hat{\mathbf{V}}^{\mathsf{H}})\,|\,(I_n \otimes \hat{\mathbf{V}}^{\mathsf{T}})] \quad (92)
$$

which satisfies the necessary and sufficient condition given by (16) in Appendix A. According to Proposition 1, the constrained sensitivity matrix of the CSI-quantized MIMO system is given by

$$
\mathbf{W}_{\mathrm{c}}(\hat{\mathbf{V}}; \boldsymbol{\Sigma}_{\mathrm{H},n}) = \mathbf{V}_2^{\mathsf{H}}\mathbf{W}(\hat{\mathbf{V}}; \boldsymbol{\Sigma}_{\mathrm{H},n})\mathbf{V}_2 \qquad (93)
$$

where matrix $\mathbf{W}(\hat{\mathbf{V}}; \boldsymbol{\Sigma}_{\mathrm{H},n})$ is the unconstrained sensitivity matrix given by (37), and $\mathbf{V}_2$ is an orthonormal matrix with its columns constituting an orthonormal basis of the null space $\mathcal{N}((\partial/\partial\mathbf{v})\mathbf{g}_1(\mathbf{v}))$, which is given by

$$
\mathbf{V}_2 = I_n \otimes \hat{\mathbf{V}}_2 \qquad (94)
$$

with $\hat{\mathbf{V}}_2$ being an orthonormal matrix with its columns constituting an orthonormal basis of the null space $\mathcal{N}(\hat{\mathbf{V}}^{\mathsf{H}})$. After some manipulations, it can be shown that the constrained sensitivity matrix can be represented by the following form:

$$
\mathbf{W}_{\mathrm{c}}(\hat{\mathbf{V}}; \boldsymbol{\Sigma}_{\mathrm{H},n}) = \frac{1}{\ln 2}\left(\frac{\rho}{n}\boldsymbol{\Sigma}_{\mathrm{H},n}\left(I + \frac{\rho}{n}\boldsymbol{\Sigma}_{\mathrm{H},n}\right)^{-1}\right) \otimes I_{(t-n)}. \qquad (95)
$$

By substituting (95) into (17), the normalized inertia profile can be obtained

$$
\begin{aligned}
&\tilde{I}_{\mathrm{c,opt}}(\hat{\mathbf{V}}; \boldsymbol{\Sigma}_{\mathrm{H},n}) \\
&= \frac{(tn - n^2)((tn - n^2)!)^{1/(tn-n^2)}\left|\frac{\rho}{n}\boldsymbol{\Sigma}_{\mathrm{H},n}\right|^{1/(tn-n^2)}}{\ln 2 \cdot (tn - n^2 + 1)\pi \left|I + \frac{\rho}{n}\boldsymbol{\Sigma}_{\mathrm{H},n}\right|^{1/(tn-n^2)}}. \quad (96)
\end{aligned}
$$

APPENDIX D
DERIVATION OF THE PROBABILITY DENSITY FUNCTION $p(\mathbf{V})$

The statistical properties of matrix $\mathbf{V}$ are discussed in this section. First, the set of all $t \times n$ $(t \ge n)$ complex matrices with orthonormal columns is called the complex Stiefel manifold, denoted as $\mathcal{V}_{n,t} = \{\mathbf{V} : \mathbf{V}^{\mathsf{H}}\mathbf{V} = I_n\}$. The volume of the complex Stiefel manifold is found in [39], which is given by

$$
\mathrm{Vol}(\mathcal{V}_{n,t}) = \int_{\mathcal{V}_{n,t}} d\mathbf{V} = \frac{2^n \pi^{nt}}{\tilde{\Gamma}_n(t)} \qquad (97)
$$

where $\tilde{\Gamma}_n(\cdot)$ is the complex multivariate gamma function given by $\tilde{\Gamma}_n(t) = \pi^{n(n-1)/2} \prod_{k=1}^{n} \Gamma(t - k + 1)$. Therefore, for random matrix $\mathbf{V}$ uniformly distributed over $\mathcal{V}_{n,t}$, the joint density function for $\mathbf{V}$ is simply given by the following form:

$$p(\mathbf{V}) = \text{Vol}(\mathcal{V}_{n,t})^{-1}, \qquad \mathbf{V} \in \mathcal{V}_{n,t}. \tag{98}$$

Since we are interested in the case of constrained source variables, where $\mathbf{V}$ is subject to constrained condition (35), the joint density function given by (98) cannot be directly applied. If we denote the constrained source space by $\mathbb{Q}$, then the complex Stiefel manifold $\mathbf{V}_{n,t}$ can be represented by expanding space $\mathbb{Q}$ under a unitary rotation $\mathbf{Q}_\text{R}$, given by

$$\mathcal{V}_{n,t} = \{\mathbf{V}\mathbf{Q}_\text{R} : \mathbf{V} \in \mathbb{Q}, \mathbf{Q}_\text{R} \in \mathcal{V}_{n,n}\}. \tag{99}$$

Therefore, the probability density function of the constrained source $\mathbf{V}$ is given by

$$\begin{aligned} p(\mathbf{V}) &= \int_{\mathcal{V}_{n,n}} \text{Vol}(\mathcal{V}_{n,t})^{-1} d\mathbf{Q}_\text{R} \\ &= \frac{\text{Vol}(\mathcal{V}_{n,n})}{\text{Vol}(\mathcal{V}_{n,t})} \\ &= \frac{\tilde{\Gamma}_n(t)}{\pi^{nt-n^2}\tilde{\Gamma}_n(n)}, \quad \mathbf{V} \in \mathcal{V}_{n,t}, \quad \mathbf{g}(\mathbf{V}) = \mathbf{0}. \end{aligned} \tag{100}$$

APPENDIX E
DERIVATION OF THE CLOSED FORM OF COEFFICIENT β_2

When the elements of the channel matrix $\mathbf{H}$ are i.i.d. complex Gaussian distributed with zero mean and unit variance, it was shown in [37] that the probability density function of the maximum eigenvalue λ_1 of the Wishart matrix $\mathbf{H}^\text{H}\mathbf{H}$ is given by the following form:

$$f_{\lambda_1}(u) = \frac{1}{\prod_{i=1}^{m}(m-i)!(l-i)!} \left(\frac{d}{du}\det(\mathbf{S}(u)) \right) \tag{101}$$

where $m = \min(t, r)$ and $l = \max(t, r)$. Matrix $\mathbf{S}(u)$ is an $m \times m$ Hankel matrix with its $(i, j)^\text{th}$ element given by $S_{i,j}(u) = \Gamma(l - m + i + j - 1, u)$, where the incomplete gamma function $\Gamma(k+1, u)$ for $k = 0, 1, 2, \ldots$, and $u > 0$ has the representation

$$\begin{aligned} \Gamma(k + 1, u) &= \int_0^u x^k \exp(-x) dx \\ &= k! \left(1 - e^{-u} \sum_{i=0}^{k} \frac{u^i}{i!} \right). \end{aligned} \tag{102}$$

The density function $f_{\lambda_1}(u)$ can be written as a finite linear combination of elementary gamma pdfs, i.e.,

$$f_{\lambda_1}(u) = \sum_{i=1}^{m} \sum_{j=l-m}^{(l+m)i-2i^2} d_{i,j} \left(\frac{i^{j+1}u^j e^{-iu}}{j!} \right)$$

$$d_{i,j} = \frac{j!c_{i,j}}{i^{j+1}\left(\prod_{i=1}^{m}(m-i)!(l-i)!\right)} \tag{103}$$

where $c_{i,j}$ is the coefficient of in front of term $e^{-iu}u^j$ when expanding the matrix determinant $|\mathbf{S}(u)|$. By substituting the density function $f_{\lambda_1}(u)$ into the expectation of β_2, one can obtain the following result:

$$\begin{aligned} \beta_2 &= \int_0^\infty \left(\frac{\rho u}{1 + \rho u} \right) f_{\lambda_1}(u) du \\ &= \sum_{i=1}^{m} \sum_{j=l-m}^{(l+m)i-2i^2} d_{i,j} \left(\frac{(j+1)\rho}{i} \right) {}_2F_0\left(j+2, 1; ; -\frac{\rho}{i}\right). \end{aligned} \tag{104}$$

REFERENCES

[1] K. K. Mukkavilli, A. Sabharwal, E. Erkip, and B. Aazhang, "On beamforming with finite rate feedback in multiple-antenna systems," *IEEE Trans. Inf. Theory*, vol. 49, no. 10, pp. 2562–2579, Oct. 2003.

[2] D. J. Love, R. W. Heath, Jr., and T. Strohmer, "Grassmannian beamforming for multiple-input multiple-output wireless systems," *IEEE Trans. Inf. Theory*, vol. 49, no. 10, pp. 2735–2747, Oct. 2003.

[3] D. J. Love and R. W. Heath, Jr., "Limited feedback unitary precoding for orthogonal space-time block codes," *IEEE Trans. Signal Process.*, vol. 53, no. 1, pp. 64–73, Jan. 2005.

[4] A. D. Dabbagh and D. J. Love, "Feedback rate-capacity loss tradeoff for limited feedback MIMO systems," *IEEE Trans. Inf. Theory*, vol. 52, no. 5, pp. 2190–2202, May 2006.

[5] J. H. Conway, R. H. Hardin, and N. J. A. Sloane, "Packing lines, planes, etc.: Packings in Grassmannian space," *Experimental Math.*, vol. 5, pp. 139–159, 1996.

[6] W. Dai, Y. Liu, and B. Rider, "Quantization bounds on Grassmann manifolds of arbitrary dimensions and MIMO communications with feedback," in *Proc. IEEE Global Telecommun. Conf. (IEEE GLOBECOM)*, St. Louis, MO, Nov. 2005, vol. 3, pp. 1456–1460.

[7] D. J. Love and R. W. Heath, Jr., "Equal gain transmission in multiple-input multiple-output wireless systems," *IEEE Trans. Commun.*, vol. 51, no. 7, pp. 1102–1110, Jul. 2003.

[8] C. R. Murthy and B. D. Rao, "Quantization methods for equal gain transmission with finite rate feedback," *IEEE Trans. Signal Process.*, vol. 55, no. 1, pp. 233–245, Jan. 2007.

[9] P. Xia, S. Zhou, and G. B. Giannakis, "Multiantenna adaptive modulation with beamforming based on bandwidth- constrained feedback," *IEEE Trans. Commun.*, vol. 53, no. 3, pp. 526–536, Mar. 2005.

[10] P. Xia and G. B. Giannakis, "Design and analysis of transmit-beamforming based on limited-rate feedback," *IEEE Trans. Signal Process.*, vol. 54, no. 5, pp. 1853–1863, May 2006.

[11] S. Zhou, Z. Wang, and G. B. Giannakis, "Quantifying the power-loss when transmit-beamforming relies on finite rate feedback," *IEEE Trans. Wirel. Commun.*, vol. 4, no. 7, pp. 1948–1957, Jul. 2005.

[12] J. Roh and B. D. Rao, "Transmit beamforming in multiple antenna systems with finite rate feedback: A VQ-based approach," *IEEE Trans. Inf. Theory*, vol. 52, no. 3, pp. 1101–1112, Mar. 2006.

[13] A. Gersho and R. M. Gray, *Vector Quantization and Signal Compression*. Norwell, MA: Kluwer Academic, 1992.

[14] J. C. Roh and B. D. Rao, "Design and analysis of MIMO spatial multiplexing systems with quantized feedback," *IEEE Trans. Signal Process.*, vol. 54, no. 8, pp. 2874–2886, Aug. 2006.

[15] J. Roh, "Multiple-antenna communication with finite rate feedback," Ph.D. dissertation, Electr. Comput. Eng. Dept., Univ. California, San Diego, 2005.

[16] A. Narula, M. J. Lopez, M. D. Trott, and G. W. Wornell, "Efficient use of side information in multiple-antenna data transmission over fading channels," *IEEE J. Sel. Areas Commun.*, vol. 16, no. 10, pp. 1423–1436, Oct. 1998.

[17] D. J. Love and R. W. Heath, Jr., "Grassmannian beamforming on correlated MIMO channels," in *IEEE GLOBECOM*, Dallas, TX, Dec. 2004, vol. 1, pp. 106–110.

[18] K. N. Lau, Y. Liu, and T. A. Chen, "On the design of MIMO block-fading channels with feedback-link capacity constraint," *IEEE Trans. Commun.*, vol. 52, no. 1, pp. 62–70, Jan. 2004.

[19] M. Skoglund and G. Jongren, "On the capacity of a multiple-antenna communication link with channel side information," *IEEE J. Sel. Areas Commun.*, vol. 21, no. 3, pp. 395–405, Apr. 2003.

[20] E. N. Onggosanusi, A. Gatherer, A. G. Dabak, and S. Hosur, "Performance analysis of closed-loop transmit diversity in the presence of feedback delay," *IEEE Trans. Commun.*, vol. 49, no. 9, pp. 1618–1630, Sep. 2001.

[21] J. Zheng, E. R. Duni, and B. D. Rao, "Analysis of multiple antenna systems with finite rate feedback using high resolution quantization theory," *IEEE Trans. Signal Process.*, vol. 55, no. 4, pp. 1461–1476, Apr. 2007.

[22] W. R. Bennett, "Spectra of quantized signals," *Bell Syst. Tech. J.*, vol. 27, pp. 446–472, Jul. 1948.

[23] A. Gersho, "Asymptotically optimal block quantization," *IEEE Trans. Inf. Theory*, vol. 25, no. 4, pp. 373–380, Jul. 1979.

[24] W. R. Gardner and B. D. Rao, "Theoretical analysis of the high-rate vector quantization of LPC parameters," *IEEE Trans. Speech Audio Process.*, vol. 3, no. 5, pp. 367–381, Sep. 1995.

[25] J. Zheng and B. D. Rao, "Analysis of multiple antenna systems with finite-rate channel information feedback over spatially correlated fading channels," *IEEE Trans. Signal Process.*, vol. 55, no. 9, pp. 4612–4626, Sep. 2007.

[26] J. Zheng and B. D. Rao, "Analysis of vector quantizers using transformed codebook with application to feedback-based multiple antenna systems," *Euro. Assoc. Signal Process. (EURASIP)*, to be published.

[27] B. Mondal, S. Dutta, and R. W. Heath, "Quantization on the complex projective space," in *Proc. IEEE Data Compression Conf.*, Snowbird, UT, Mar. 2006, pp. 242–251.

[28] J. Zheng and B. D. Rao, "Analysis of mimo systems with finite-rate channel state information feedback," in *Proc. 40th Asilomar Conf. Signals, Syst. Comput.*, Pacific Grove, CA, Oct. 2006, pp. 1521–1525.

[29] J. Zheng, "Design and analysis of multiple antenna communication systems with finite rate feedback," Ph.D. dissertation, Electr. Comput. Eng. Dept., Univ. California, San Diego, 2006.

[30] T. K. Y. Lo, "Maximum ratio transmission," *IEEE Trans. Commun.*, vol. 47, no. 10, pp. 1458–1461, Oct. 1999.

[31] R. Remmert, *Theory of Complex Functions*. New York: Springer-Verlag, 1991.

[32] K. Kreutz-Delgado, "Lecture supplement on complex vector calculus," Apr. 2006 [Online]. Available: http://dsp.ucsd.edu/~kreutz/PEI05.html

[33] R. M. Gray, *Source Coding Theory*. Norwell, MA: Kluwer, 1990.

[34] J. Conway and N. Sloane, "Voronoi regions of lattices, second moments of polytopes, and quantization," *IEEE Trans. Inf. Theory*, vol. IT-28, no. 2, pp. 211–226, Mar. 1982.

[35] D. J. Love and R. W. Heath, Jr., "Multi-mode precoding for MIMO wireless systems," *IEEE Trans. Signal Process.*, to be published.

[36] R. J. Muirhead, *Aspects of Multivariate Statistical Theory*. New York: Wiley, 1982.

[37] P. A. Dighe, R. K. Mallik, and S. S. Jamuar, "Analysis of transmit-receive diversity in Rayleigh fading," *IEEE Trans. Commun.*, vol. 51, no. 4, pp. 694–703, Apr. 2003.

[38] I. S. Gradshteyn and I. M. Ryzhik, *Table of Integrals, Series and Products*, 5th ed. San Diego, CA: Academic, 1994.

[39] A. Edelman, "Eigenvalues and condition numbers of random matrices," Ph.D. dissertation, Dept. Math., Massachusetts Inst. Technol., Cambridge, MA, 1989.
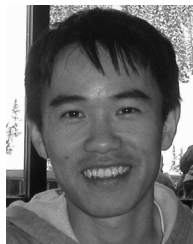
Jun Zheng (S'04) received the B.S. degree in electrical engineering from Tsinghua University, Beijing, China, in 2001, the M.S. degree in electrical engineering from Texas A&M University, College Station, in 2003, and the Ph.D. degree in electrical and computer engineering from the University of California, San Diego, in 2006.

He is currently with Broadcom, Inc., San Diego, CA. His research interests include the area of communication theory, information theory, coding theory, statistical estimation theory, and their applications in multiple-input multiple-output (MIMO) and multi-carrier (OFDM) wireless communications.

Bhaskar D. Rao (S'80–M'83–SM'91–F'00) received the B.Tech. degree in electronics and electrical communication engineering from the Indian Institute of Technology, Kharagpur, India, in 1979, and the M.S. and Ph.D. degrees from the University of Southern California, Los Angeles, in 1981 and 1983, respectively.

Since 1983, he has been with the University of California at San Diego, La Jolla, where he is currently a Professor with the Electrical and Computer Engineering Department. His research interests include the areas of digital signal processing, estimation theory, and optimization theory, with applications to digital communications, speech signal processing, and human-computer interactions.

Dr. Rao has been a member of the Statistical Signal and Array Processing Technical Committee and the Signal Processing Theory and Methods Technical Committee of the IEEE Signal Processing Society. He is currently a member of the Signal Processing for Communications Technical Committee and serves on the editorial board of the *EURASIP Signal Processing Journal*.